Mesut YİĞİT, M.D.

Principal Investigator (PI)
Prof. Dr. Caner SÜSAL

KOÇ ÜNİVERSİTESİ

TIREX
KOÇ UNIVERSITY TRANSPLANT IMMUNOLOGY RESEARCH CENTER OF EXCELLENCE

Funded by the European Union

DNA

Watson and Crick

760 NATURE October 24, 1953 Vol. 172

The X-ray diffraction photograph of crystalline deoxyribonucleic acid (sodium salt) is shown in Fig. 1. In view of its very complex biological functions (for example, the genetical transforming[2] of bacteria) it is remarkable that its crystallinity is so perfect, for such crystallinity indicates a large element of molecular simplicity. We have found no difference in the diffraction patterns of crystalline deoxyribonucleic acid obtained from calf thymus, mouse sarcoma, human white blood cells, *E. coli*, pneumococcus and *Paracentrotus* sperm, although the ratio of bases in the deoxyribonucleic acids varies considerably with species. These facts, combined with the irregularity of sequence of nitrogen bases[13] and the hydrogen bonding between bases[14], produce a contradiction which is only resolved by a simplifying concept such as the specific pairing of bases suggested by Watson and Crick[7].

A qualitative view of the X-ray photograph shows several main features which point clearly to the type of structure involved, but the data may be interpreted with more certainty when the reflexions are indexed and intensities measured and plotted in reciprocal space. By using a high-resolution pinhole camera, about a hundred and twenty separate reflexions were resolved in the fibre photograph. Intensities were measured using a microdensitometer. The values are preliminary.

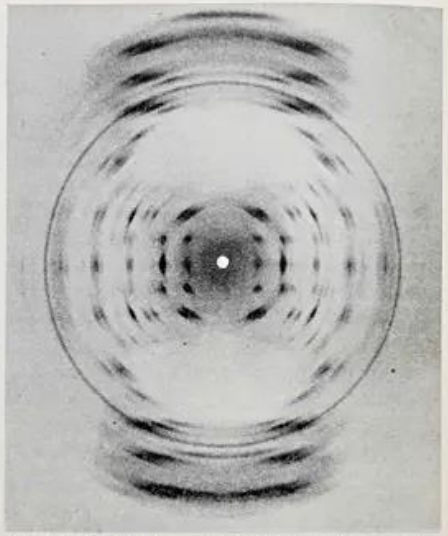

Fig. 1. X-ray diffraction photograph of a bundle of four fibres of crystalline mouse sarcoma deoxypentose nucleic acid (sodium salt) at approximately 75 per cent relative humidity. The ring is due to impurity. (Deoxypentose nucleic acid supplied by E. Barclay and L. D. Hamilton)

The unit cell of calf thymus deoxyribonucleic acid has been given[4] as face-centred monoclinic:

$a = 22{\cdot}0$ A. $b = 39{\cdot}8$ A. $c = 28{\cdot}1$ A. $\beta = 96\frac{1}{2}°$.

We find the values for mouse sarcoma deoxyribonucleic acid to be:

$a = 22{\cdot}2$ A. $b = 40{\cdot}4$ A. $c = 28{\cdot}1$ A. $\beta = 97{\cdot}1°$.

Deduction of the Main Features of the Structure

Fig. 2 shows a two-dimensional view of the intensities of reflexions plotted in reciprocal space. When reflexions overlap, the intensity is divided by the number of reciprocal lattice points possibly involved.

(*a*) *The structure is helical.* The pattern corresponds in striking fashion with the Fourier transform of a system of helices. The large empty trapezoidal space on and near the meridian strongly suggests a helix but could, however, also be given by alternative structures in which rods or sheets are inclined to the axis. These pseudo-helical structures can be distinguished, however, by the fact that they do not give several zeros of intensity on the layer lines, and the form function is not circularly symmetrical about the fibre axis. If paracrystalline deoxyribonucleic acid only were available, it would be impossible to establish the circular symmetry of the form function, and hence three-dimensional data obtained from study of the crystalline acid are necessary if the helical nature of the structure is to be proved. This is discussed later.

(*b*) *A major part of the helix has one sharply defined diameter.* The intensity distribution on the second layer line and on the outer parts of the equator alternates markedly between strong and weak and corresponds respectively with the functions J_1^2 and J_0^2 (squares of second- and zero-order Bessel functions). This diffraction would be produced by a helix of sharply defined diameter of about 18 A. The intensity on the 4th, 5th, 6th, 7th, 9th and 11th layer lines corresponds roughly to the main maxima of the functions J_4^2, J_5^2, J_6^2, J_7^2, J_9^2 and J_{11}^2 (Fig. 2), again for the same diameter of 18 A.

(*c*) *There are two coaxial 18 A. diameter helices spaced half a pitch-length apart.* The 1st and 3rd layer lines are weaker than the second, and the intensities correspond roughly with J_1^2 and J_3^2 (Fig. 2) respectively, for a helix of diameter approximately 10 A. The strong diffraction from 18 A. diameter helices observed on the 2nd layer line, but absent from 1st and 3rd, indicates that the structure contains two 18 A. diameter coaxial helices spaced apart along the fibre axis by about half the pitch-length of 28 A. (the layer line spacing) (see also ref. 8). The inner regions of the equator correspond to a smaller average diameter than 18 A., and if the 10 A. helix extends over a range of diameter from about 9 to 14 A. it will contribute mainly to the inner regions of the equator and will not affect much the outer region, which corresponds to J_0^2 of 18 A. The equatorial intensity distribution will then be accounted for by the addition of the amplitudes diffracted by the 18 and 10 A. helices (Fig. 2). The 18 A. diameter helices do not contribute J_1^2 to the 4th layer line; hence the thickness of the 18 A. helix in the axial direction must be at least 3·5 A.

(*d*) *Spaced centrally between the two 18 A. diameter helices is one helix of mean diameter about 10 A.* We expect that the 10 A. helix may contribute to the intensity of the 2nd layer line. If this intensity followed accurately a J_1^2 function, the heights of the maxima first and second closest to the centre of the layer line would be in the ratio 1 : 0·4. In fact, these heights are about equal. If a small amplitude of J_2, corresponding to 10 A. diameter, is added *out of phase* to the 18 A. J_0, such an effect would be produced (Fig. 2). Hence we expect the 10 A. diameter helix to be spaced along the helix axis *halfway* between the two 18 A. diameter helices, the whole system being coaxial. This 10 A. diameter helix is apparently that part of the structure which Franklin and Gosling have remarked[5] is not repeated 14 A. apart along the fibre axis. Indications of this single helix can, in fact, be seen on their two-dimensional Patterson diagram.

(*e*) *There are eleven nucleotides per turn of one helix.* This is deduced from the fact that there is a system of Bessel function maxima converging on the centre of the 11th layer line (see also ref. 8).

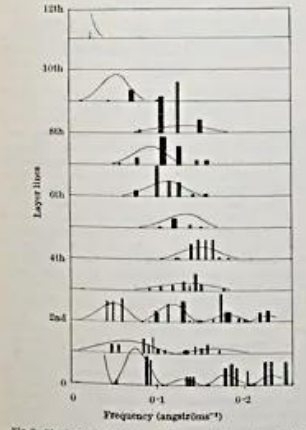

Fig. 2. Plot in reciprocal space of X-ray reflexions from crystalline deoxyribonucleic acid; fibre axis vertical. The height of each black rectangle is proportional to the observed form factor of the structure, and the area to the total intensity produced by overlapping reflexions. The continuous curve corresponds to the roughly calculated form factor for the helical structure suggested in the text

No. 4382 October 24, 1953 NATURE 761

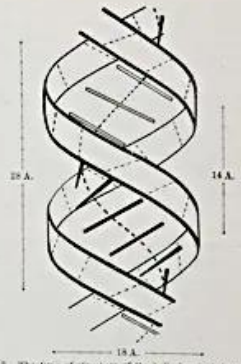

Fig. 3. The type of structure of the helical unit deduced from X-ray data of crystalline deoxyribonucleic acid. One helix of diameter approximately 10 A. is formed by a system of eleven inclined rods per turn of the helix. This helix is surrounded by two 18 A. diameter helices, each of which is also formed of eleven units per turn

(*f*) *The nucleotide shape resembles that of a rod inclined to the helix axis.* If the helical system is divided into nucleotides by planes at right angles to the helix axis, the intensities of the 10th, 9th and 8th layer lines would resemble that of the zero, 1st, 2nd and 3rd layer lines. In fact, this effect is observed in so far as the 18 A. diameter helix does contribute to the 9th layer line (though weakly) and is partly absent from the 10th. But it is anomalous that the 10 A. diameter helix does not contribute to the 10th layer line and the 18 A. helix does contribute, as J_1^2, to the 7th layer line. These effects would be explained if the nucleotides formed roughly a series of rods inclined at an angle of about 65° to the fibre axis in the opposite sense to the inclination of the helix. The X-rays are then reflected off these rods in a direction about 25° to the fibre axis. The 10 A. diameter helix, being in effect divided by inclined planes, diffracts very little energy along the meridian, and the 10th layer line is accordingly absent.

The structure of the helical system therefore begins to become clear and its probable form is shown diagrammatically in Fig. 3.

Circular Symmetry of the Form Function and the Elimination of Pseudo-Helical Structures

The fact that the form function, for example, on the 2nd layer line, alternates fairly smoothly between strong and very weak, indicates that it has circular symmetry about the fibre axis. Hence all pseudo-helical structures are eliminated. However, as the lattice is asymmetrical, a symmetrical form function is quite likely to produce general asymmetry of the intensity distribution. This effect, combined with some ambiguity of indexing, gave rise to the suggestion[3] that there might be a very definite asymmetry in the form function and therefore in the structure itself. If this were the case, the structure could not be helical unless the helix were considerably distorted. Probably the greatest asymmetry of reflected energy

Clustered Regularly Interspaced Short Palindromic Repeats (CRISPR)

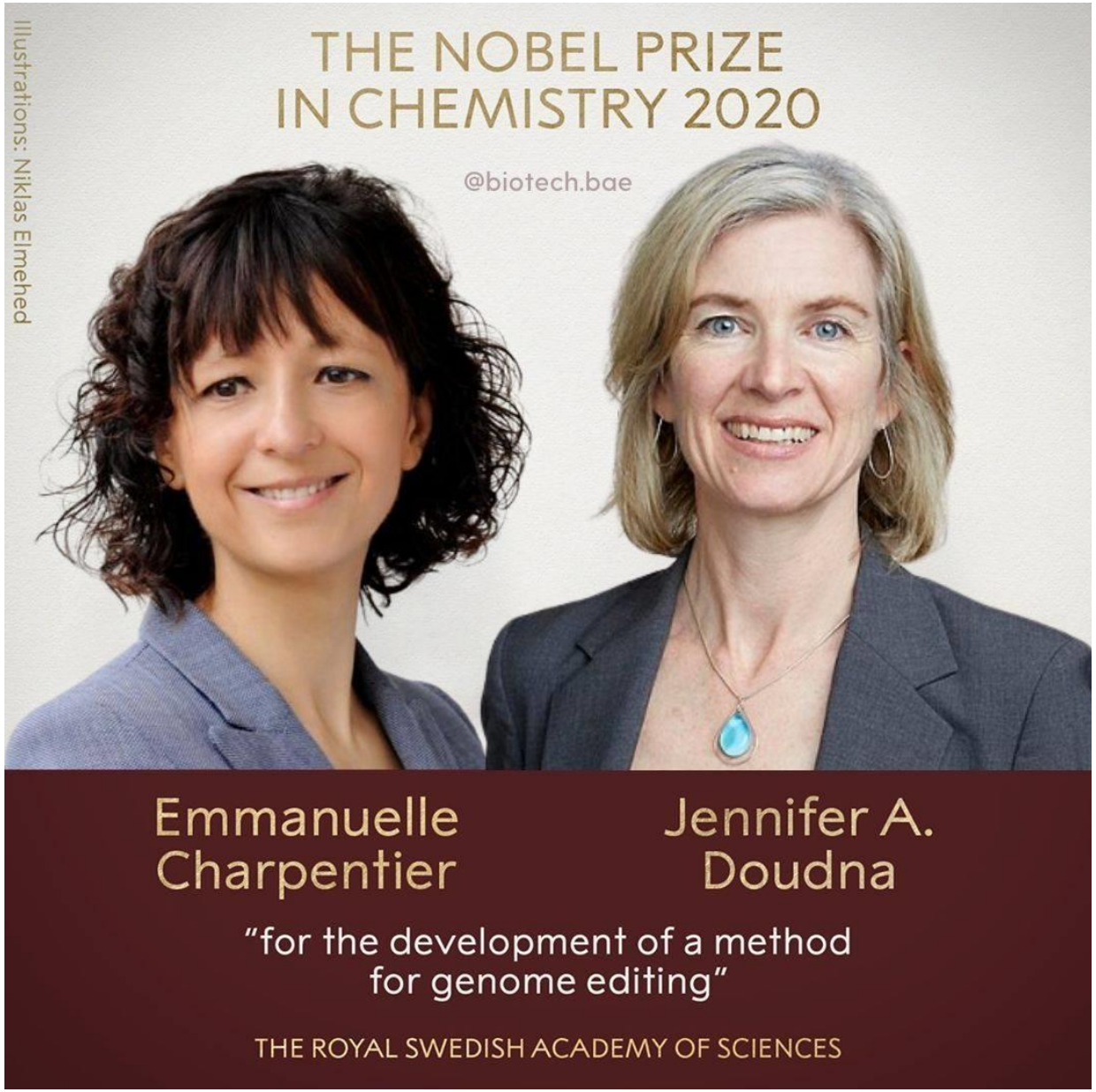

Clustered Regularly Interspaced Short Palindromic Repeats (CRISPR)

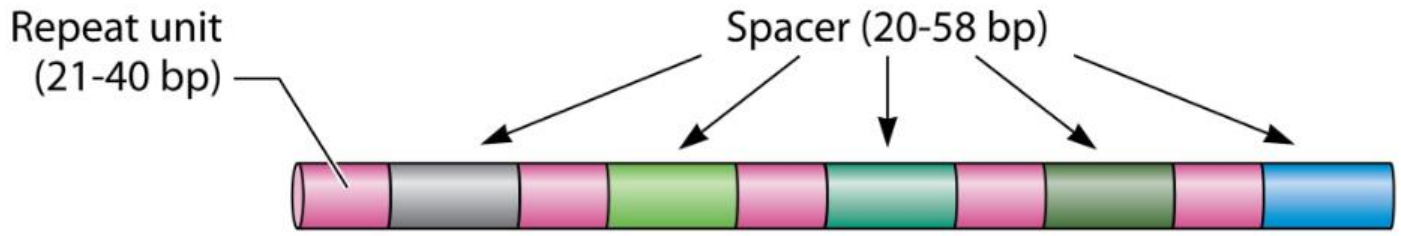

E. coli (1987)

CGGTTTATCCCCGCTGCGCGGGGAACTC

H. mediterranei (1993)

GTTACAGACGAACCCTAGTTGGGTTGAAGC

JOURNAL OF BACTERIOLOGY, Dec. 1987, p. 5429–5433
0021-9193/87/125429-05$02.00/0

Vol. 169, No. 12

Nucleotide Sequence of the *iap* Gene, Responsible for Alkaline Phosphatase Isozyme Conversion in *Escherichia coli*, and Identification of the Gene Product

YOSHIZUMI ISHINO, HIDEO SHINAGAWA, KOZO MAKINO, MITSUKO AMEMURA, AND ATSUO NAKATA*
Department of Experimental Chemotherapy, The Research Institute for Microbial Diseases, Osaka University, 3-1 Yamadaoka, Suita, Osaka 565, Japan

Received 1 May 1987/Accepted 22 August 1987

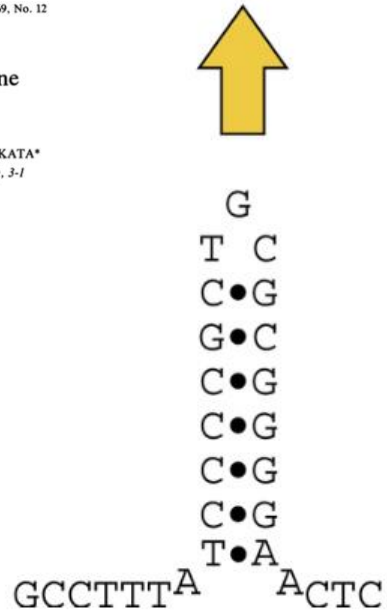

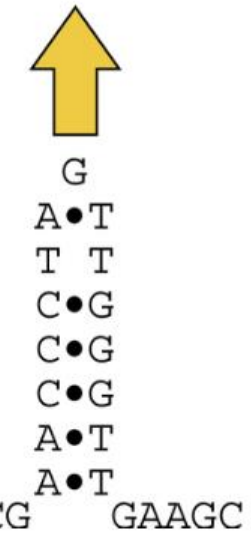

Molecular Microbiology (1993) 9(3), 613–621

Transcription at different salinities of *Haloferax mediterranei* sequences adjacent to partially modified *Pst*I sites

F. J. M. Mojica, G. Juez and F. Rodríguez-Valera*
Departamento de Genética Molecular y Microbiología, Apartado 374, Universidad de Alicante, 03080 Alicante, Spain.

involved in the high-affinity K^+ transport, whose regulation is effected at transcriptional level and is being extensively studied (Csonka, 1989; May *et al.*, 1989; Mizuno and Mizushima, 1990; Sugiura *et al.*, 1992). A role for the

Ishino et al,History of CRISPR-Cas from Encounter with a Mysterious Repeated Sequence to Genome Editing Technology,JOB,2018

Prokaryotların Adaptif Bağışıklığı: CRISPR'ın Doğuşu

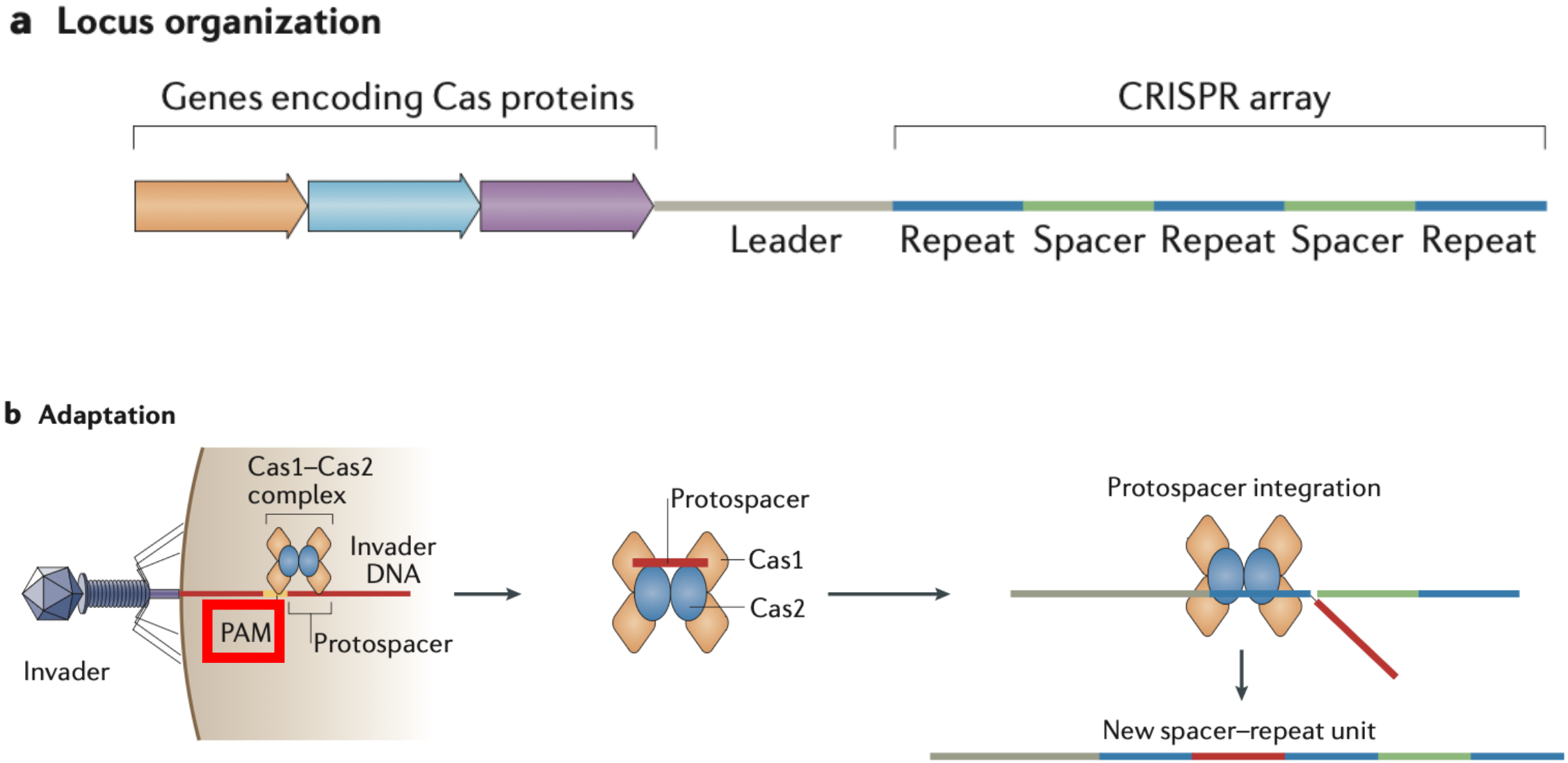

Amitai and Sorek, CRISPR–Cas adaptation: insights into the mechanism of action, Progress, 2016

Prokaryotların Adaptif Bağışıklığı: CRISPR'ın Doğuşu

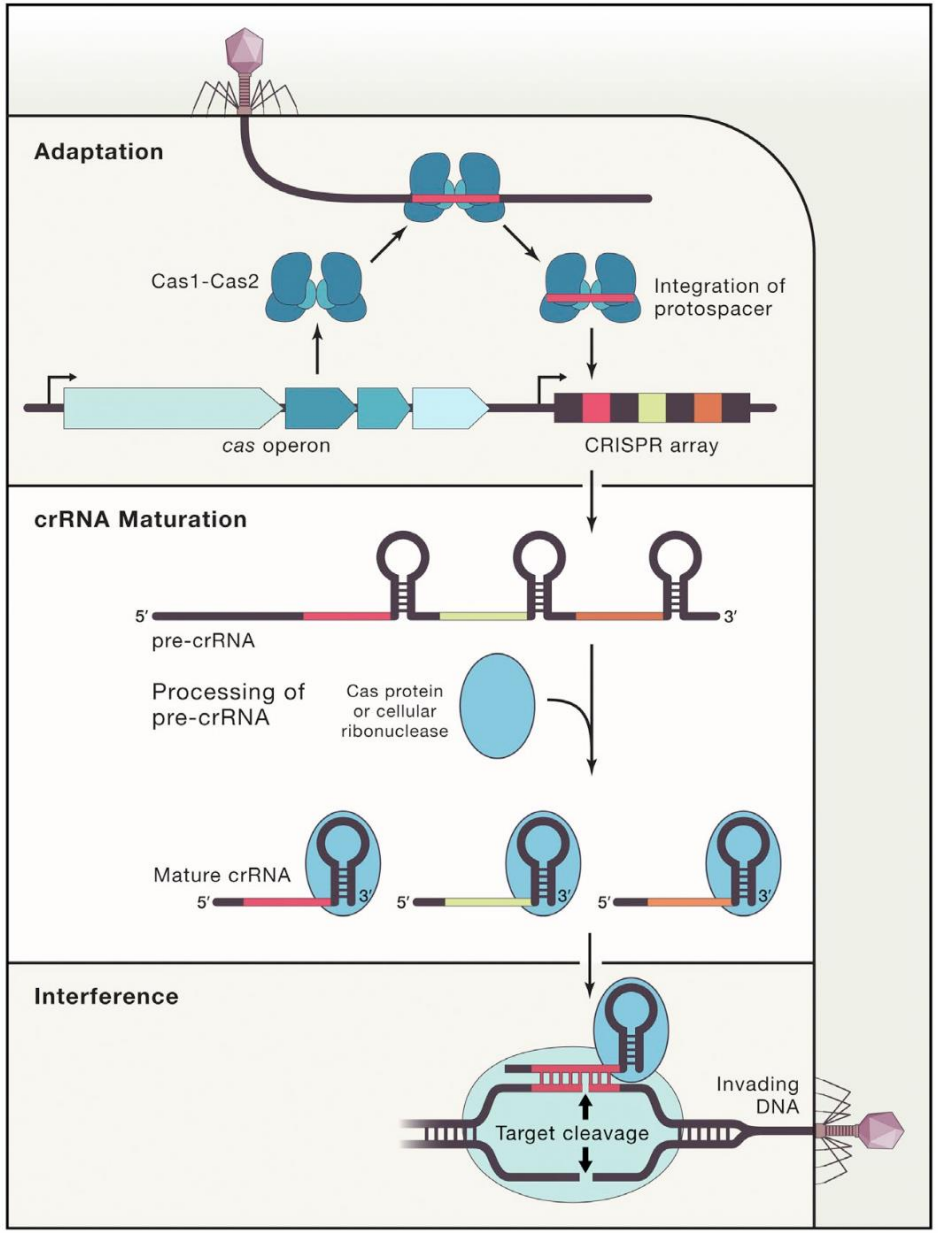

Hille et al., The Biology of CRISPR-Cas: Backward and Forward, Cell, 2018

Prokaryotların Adaptif Bağışıklığı: CRISPR'ın Doğuşu

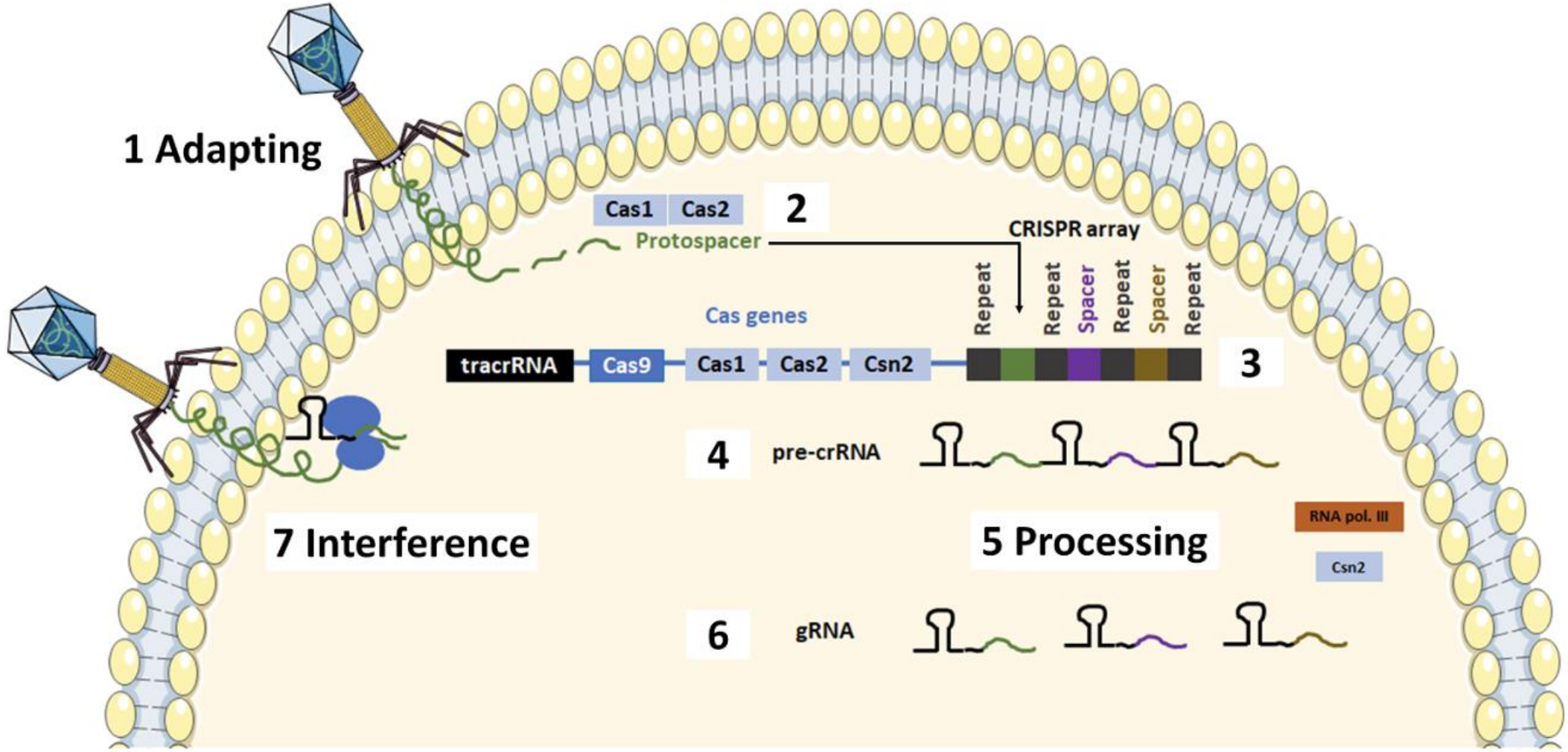

Araldi et al., Medical applications of CRISPR/Cas tool: A comprehensive overview, GENE, 2020

Pre-crRNA, cr-RNA Aand TracRNA

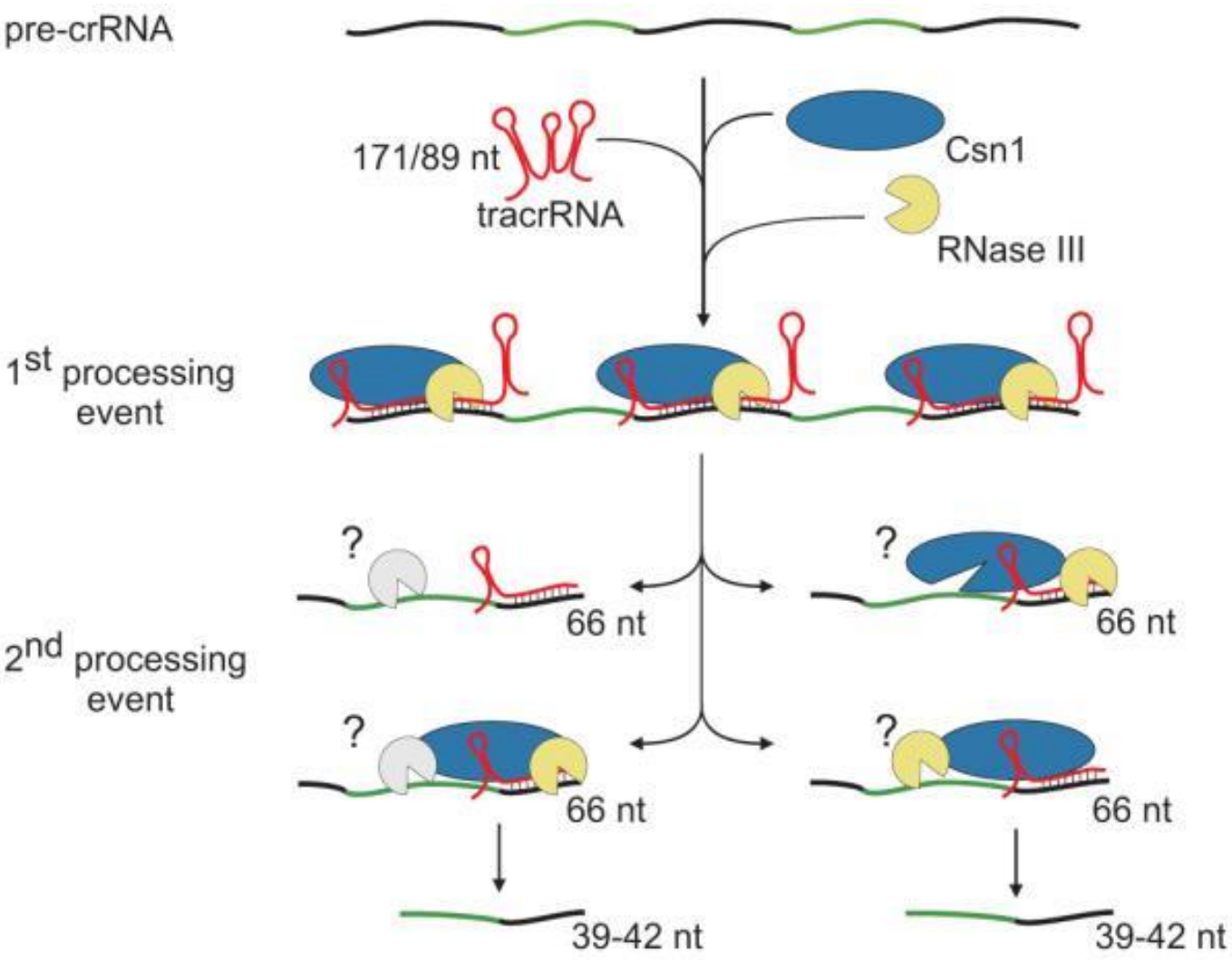

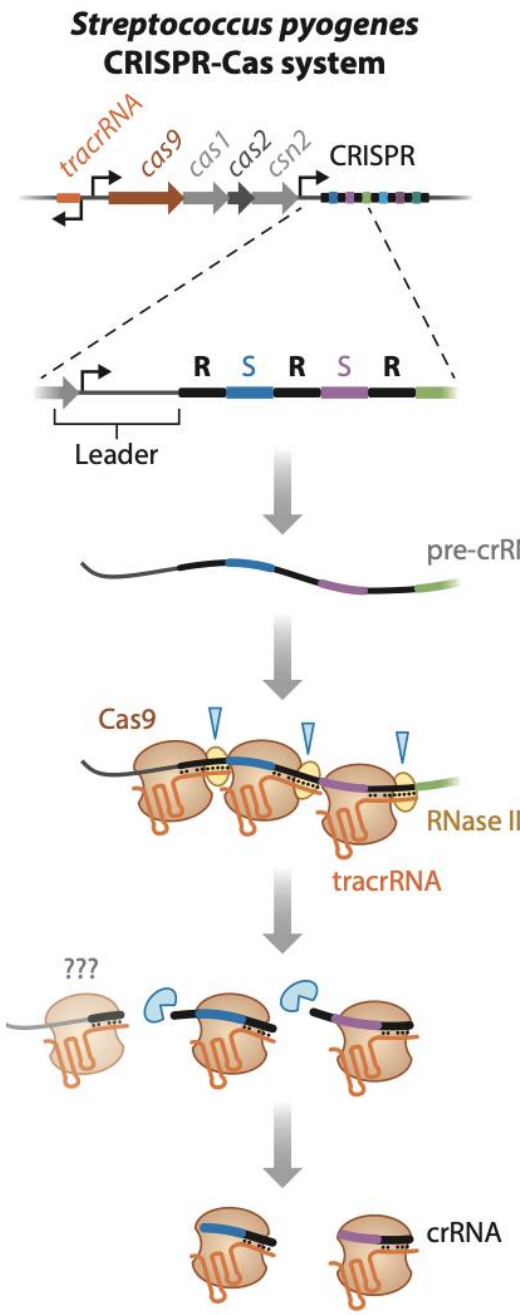

Charpentier, CRISPR RNA maturation by *trans*-encoded small RNA and host factor RNase III, Nature, 2011

Prokaryotların Adaptif Bağışıklığı: CRISPR'ın Doğuşu

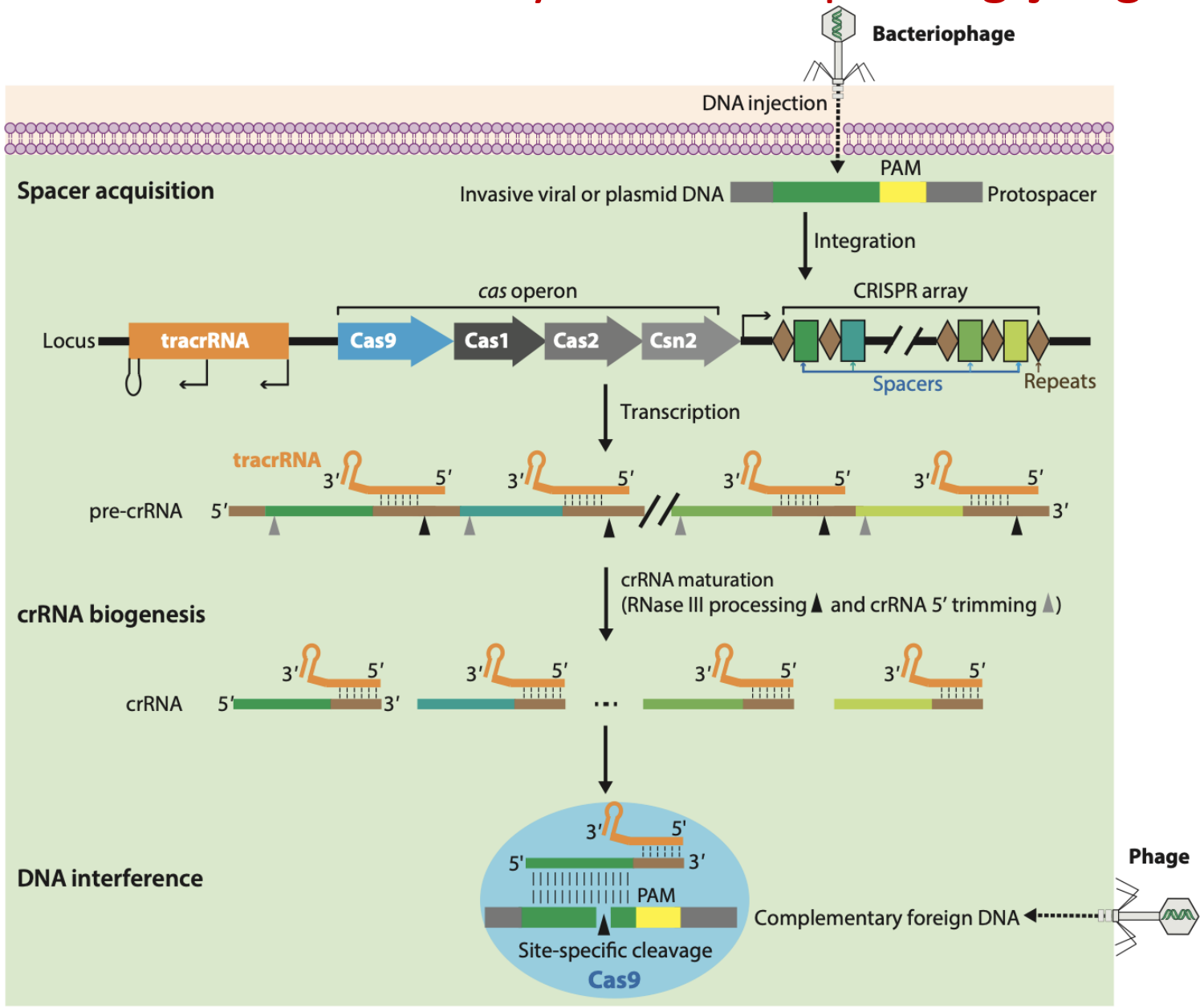

Doudna and Jiag, CRISPR–Cas9 Structures and Mechanisms, Annual Reviews, 2017

Prokaryotların Adaptif Bağışıklığı: CRISPR'ın Doğuşu

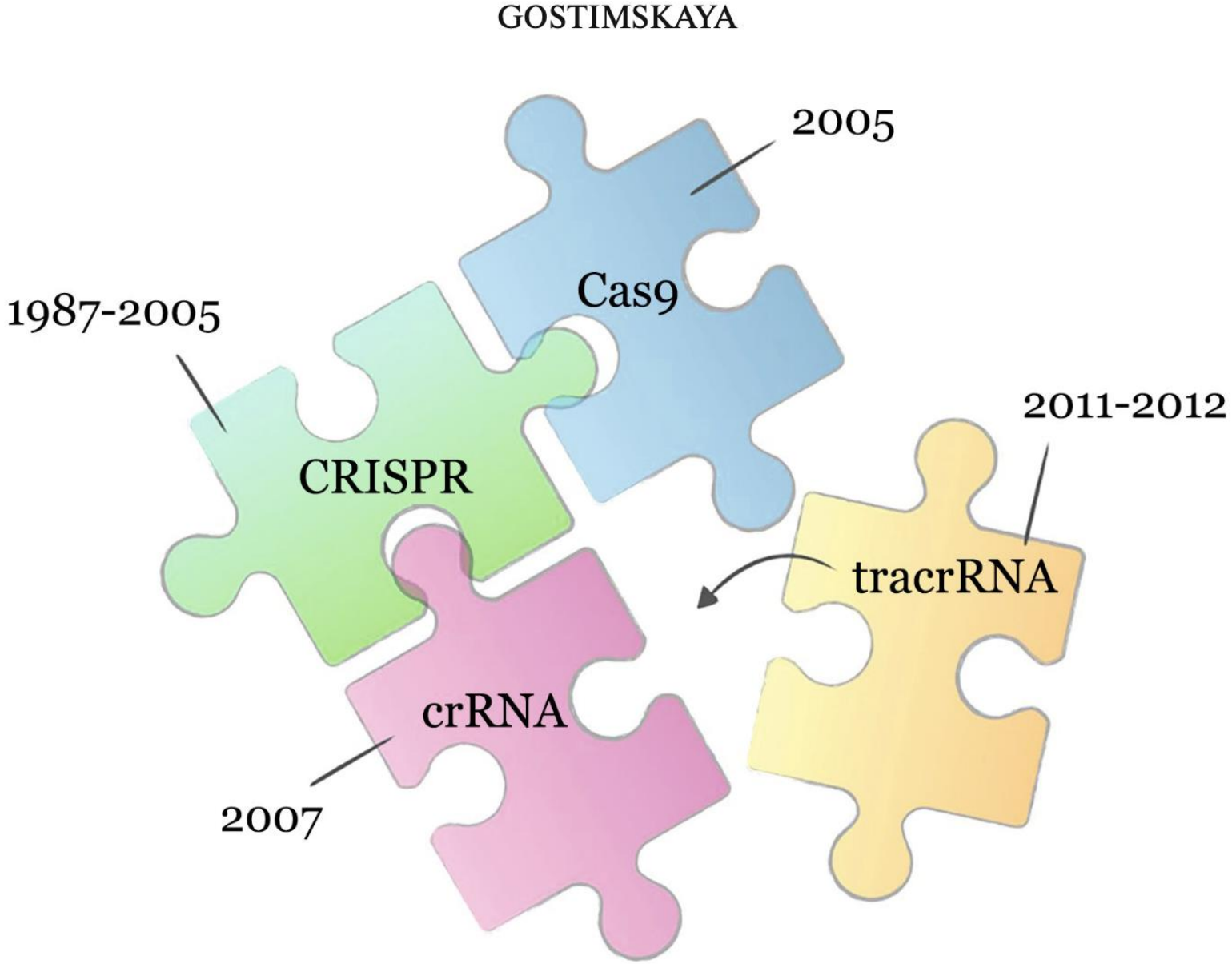

Gostimskaya, CRISPR–Cas9: A History of Its Discovery and Ethical Considerations of Its Use in Genome Editing, 2022

Bakteri Kendi DNA'sını Neden Kesmez?
Prokaryotta Otoimmünitenin Önlenmesi!

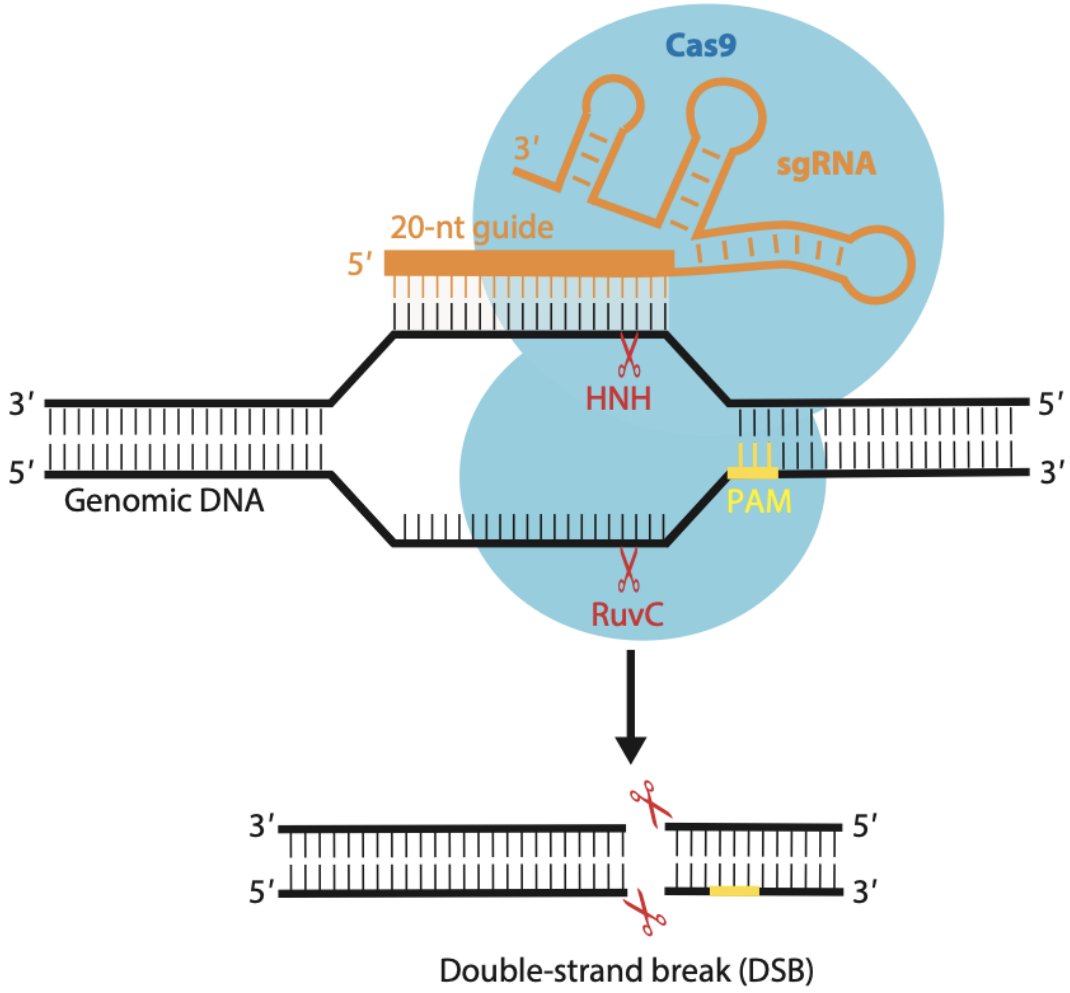

-NGG

Doudna and Jiag, CRISPR–Cas9 Structures and Mechanisms, Annual Reviews, 2017

Clustered Regularly Interspaced Short Palindromic Repeats (CRISPR)

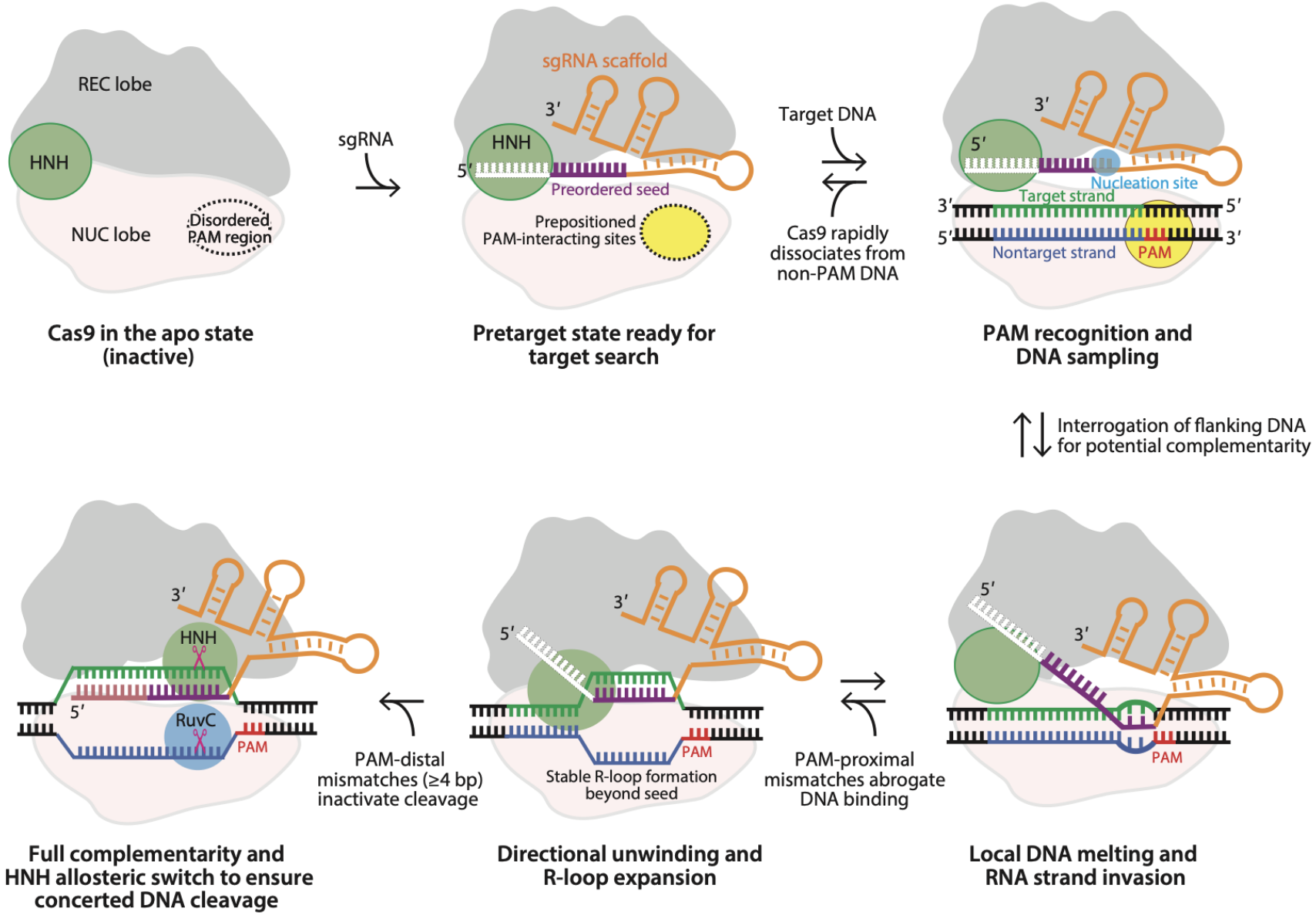

Doudna and Jiag, CRISPR–Cas9 Structures and Mechanisms, Annual Reviews, 2017

Double-Strand Break(DSB)

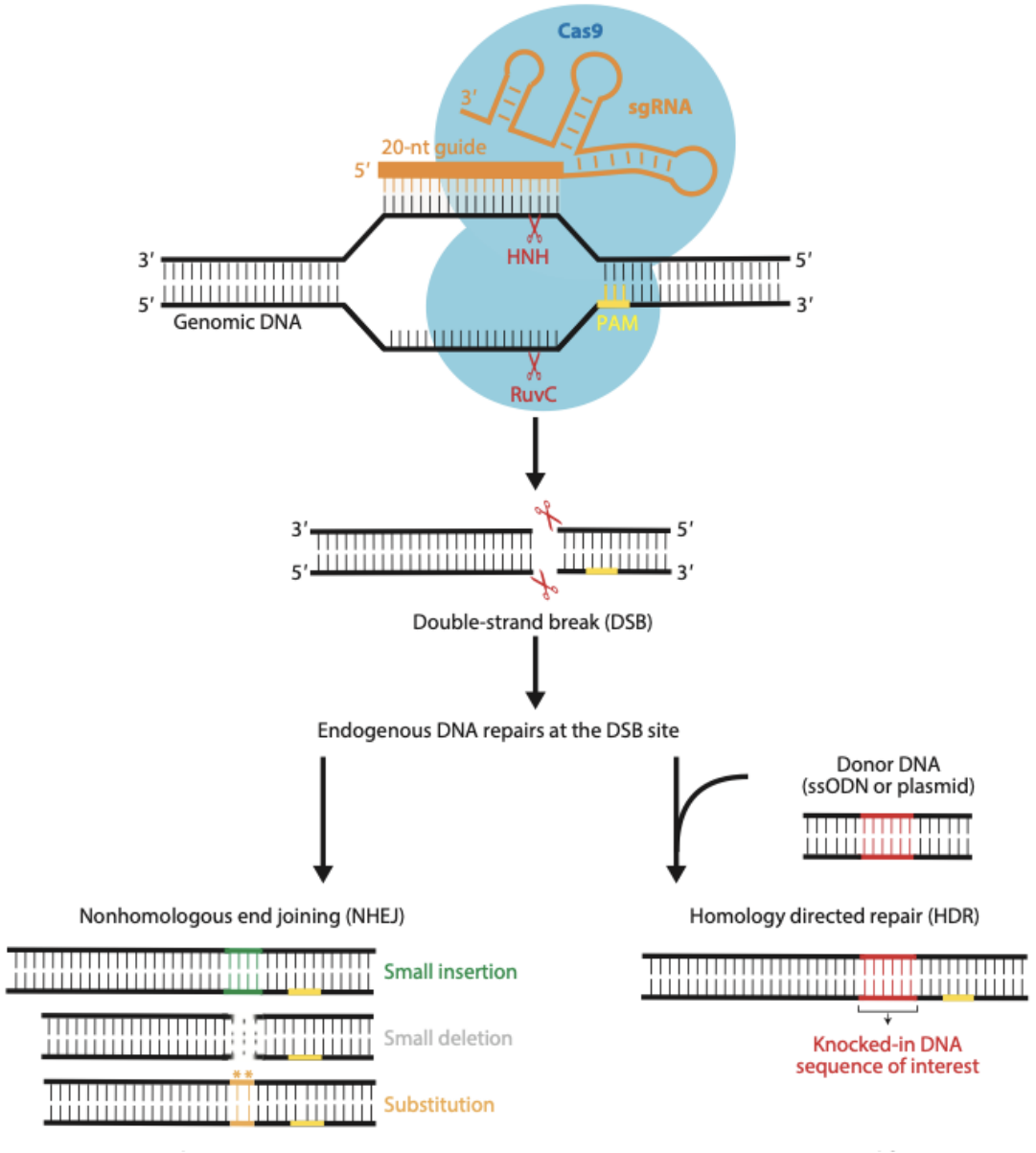

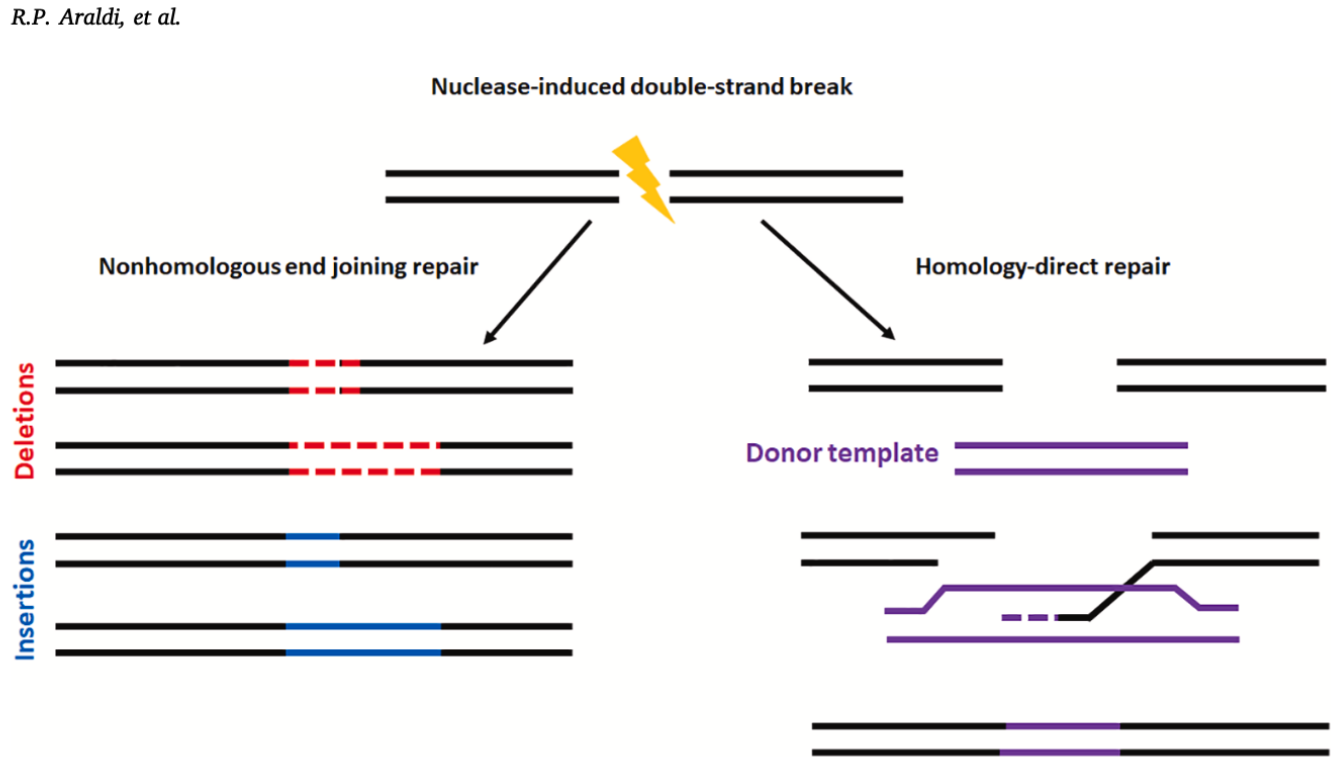

Doudna and Jiag, CRISPR–Cas9 Structures and Mechanisms, Annual Reviews, 2017

A Programmable Dual-RNA–Guided DNA Endonuclease in Adaptive Bacterial Immunity

MARTIN JINEK, KRZYSZTOF CHYLINSKI, INES FONFARA, MICHAEL HAUER, JENNIFER A. DOUDNA, AND EMMANUELLE CHARPENTIER Authors Info & Affiliations

SCIENCE • 28 Jun 2012 • Vol 337, Issue 6096 • pp. 816-821 • DOI: 10.1126/science.1225829

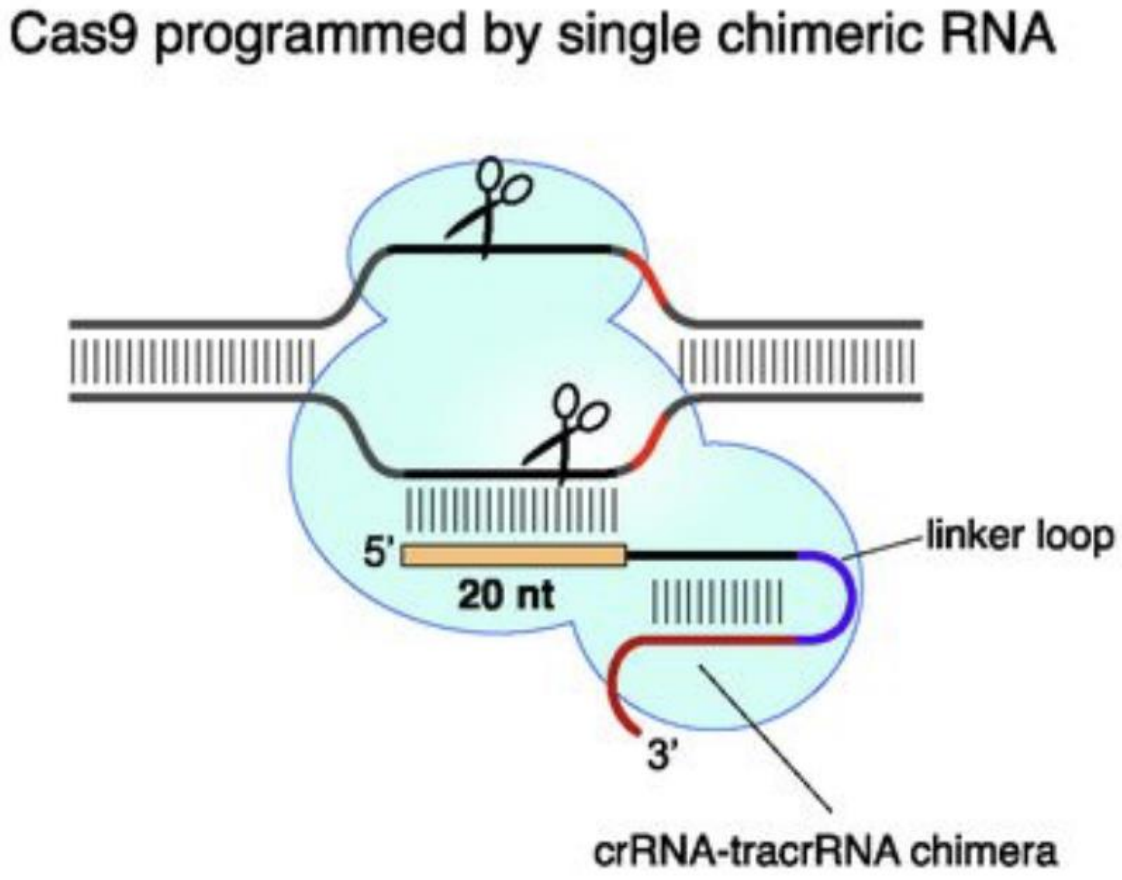

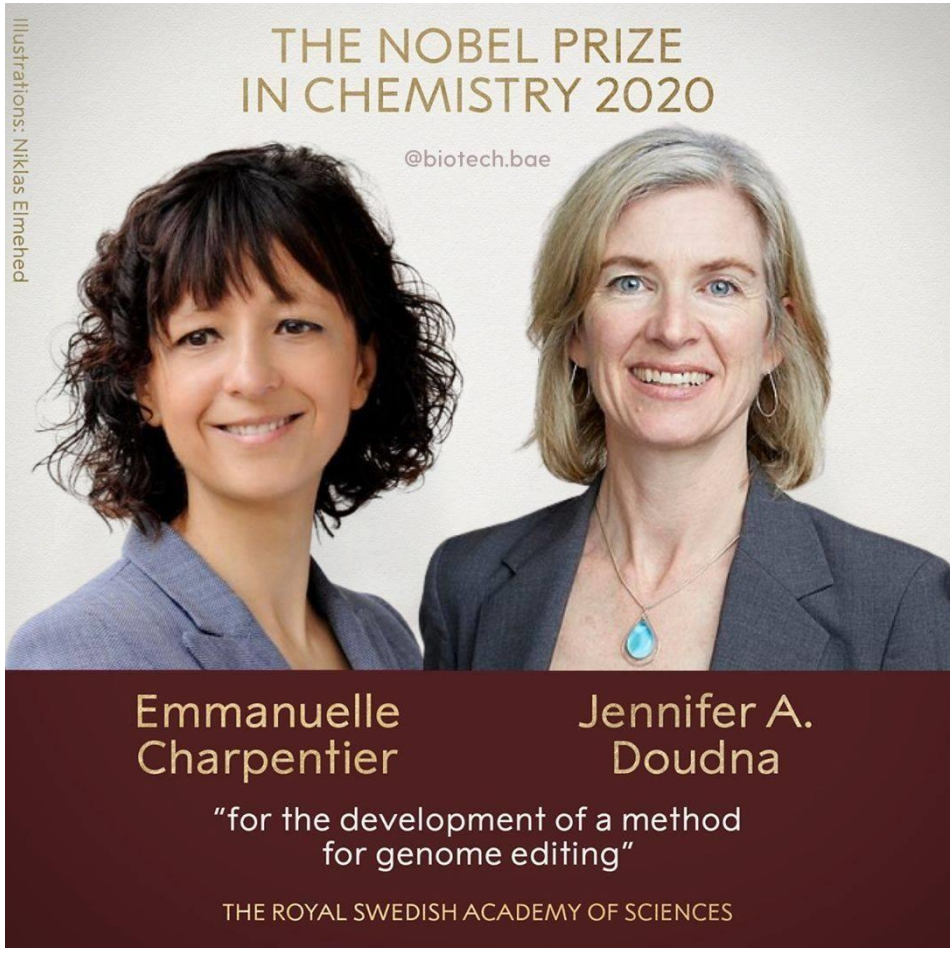

HLA-I Knock-Out

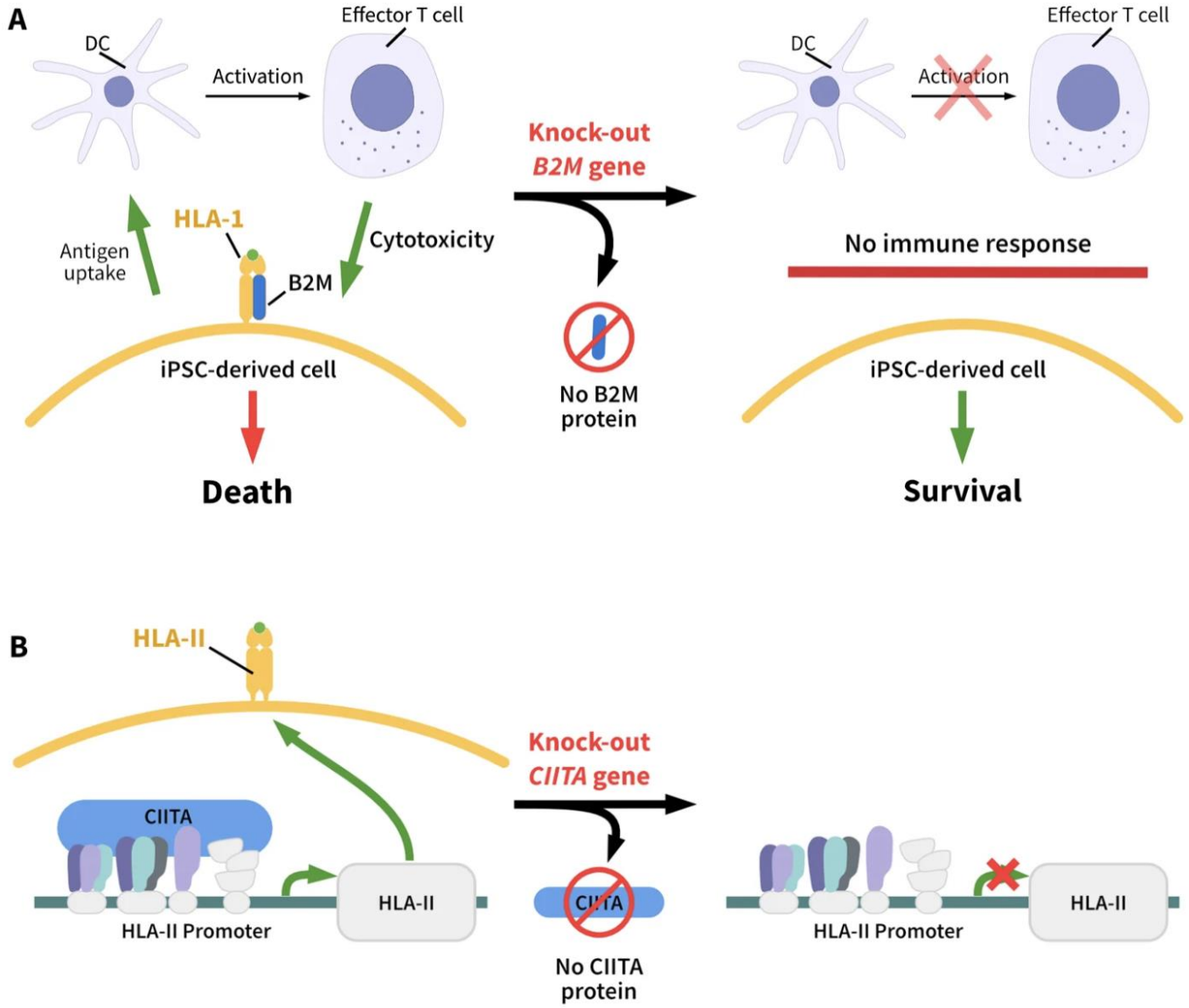

*Sarah Eminli-Meissner PhD, Editing B2M and CIITA to Create Hypoimmune Cell Lines for Cell Therapy, REPROCELL, 2023

HLA-I Knock-Out via Lentivirus

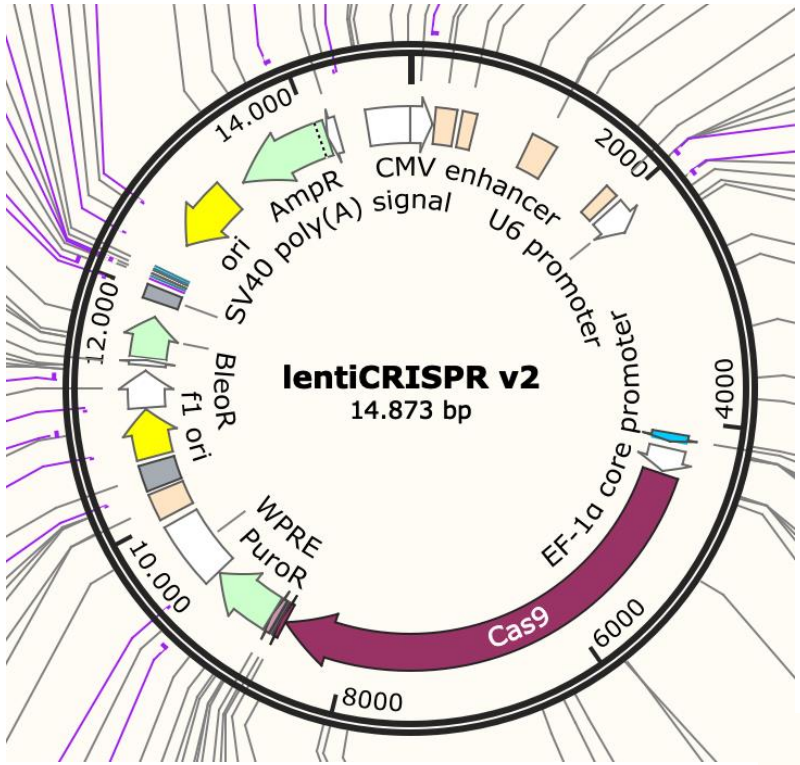

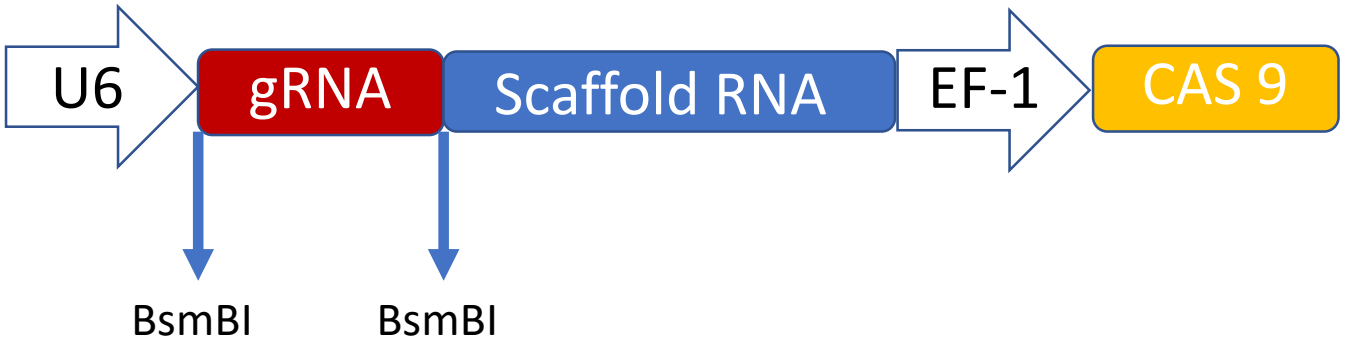

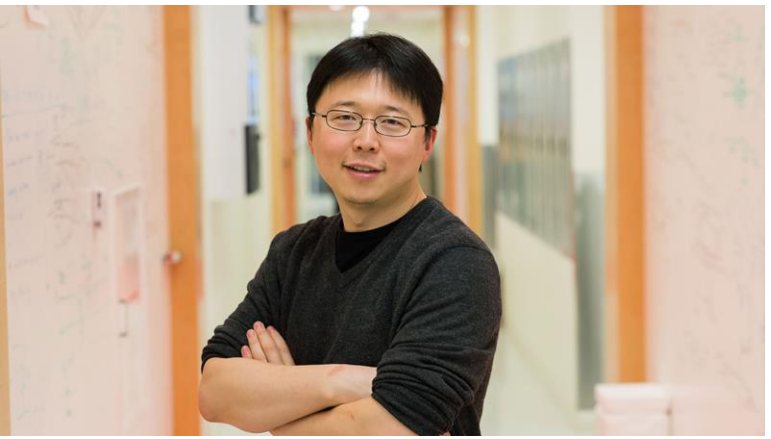

Feng Zhang, MIT

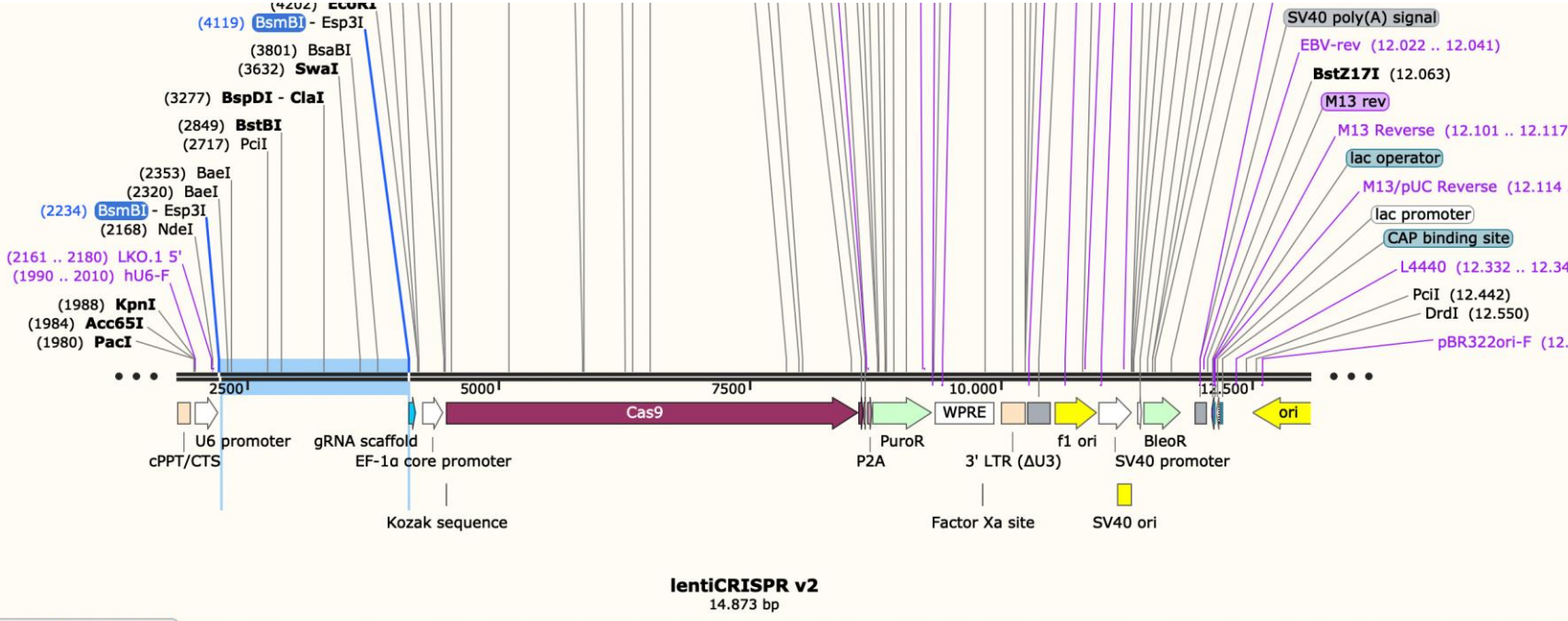

HLA-I Knock-Out via Lentivirus

Predesigned Alt-R™ CRISPR-Cas9 guide RNA

Select from predesigned Alt-R CRISPR-Cas9 guide RNAs (gRNAs, such as crRNA and sgRNA) targeting human, mouse, rat, zebrafish, or *C. elegans* gene targets.
For HDR experiment designs, please see the following HDR design tool.

Search for predesigned gRNA | Design custom gRNA | CRISPR-Cas9 gRNA checker

Species: Homo sapiens
Input format: Gene symbol
Designs per gene: 6

SEARCH
CLEAR AND RESET

Paste/Type input | Upload file

Enter up to 100, separated by commas.

B2M

Design ID: Hs.Cas9.B2M.1.AB B2M ✔ RECOMMENDED — **Predesigned Alt-R CRISPR-Cas9 gRNA**

Position	Strand	Sequence	PAM	On-target score	Off-target score
44715511	-	AAGTCAACTTCAATGTCGGA	TGG	91	70

Show off-target details + | Show related products

+ ADD TO DESIGN SET

HLA-I Knock-Out via Lentivirus

Oligo 1: Oligo 1

5′ CACCGGCTACTCTCTCTTTCTGGCC

5′ Phosphorylated

Oligo 2: Oligo 2

5′ AAACGGCCAGAAAGAGAGAGTAGCC

5′ Phosphorylated

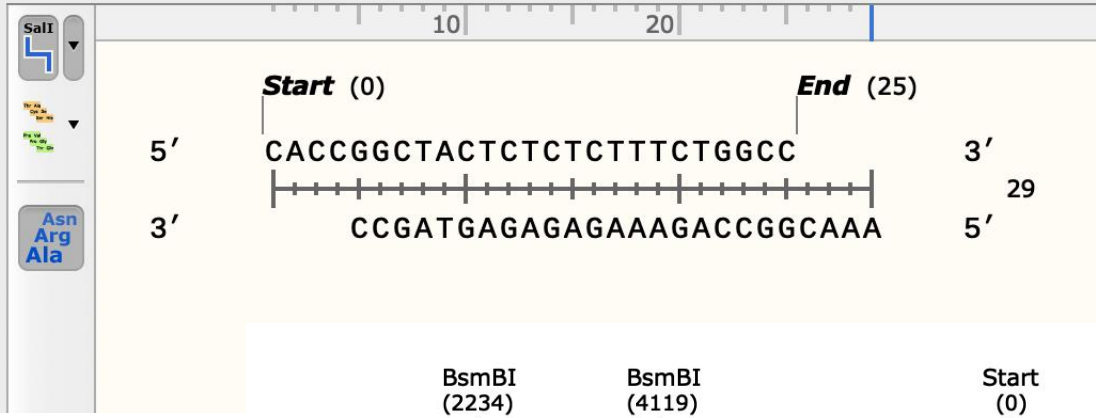

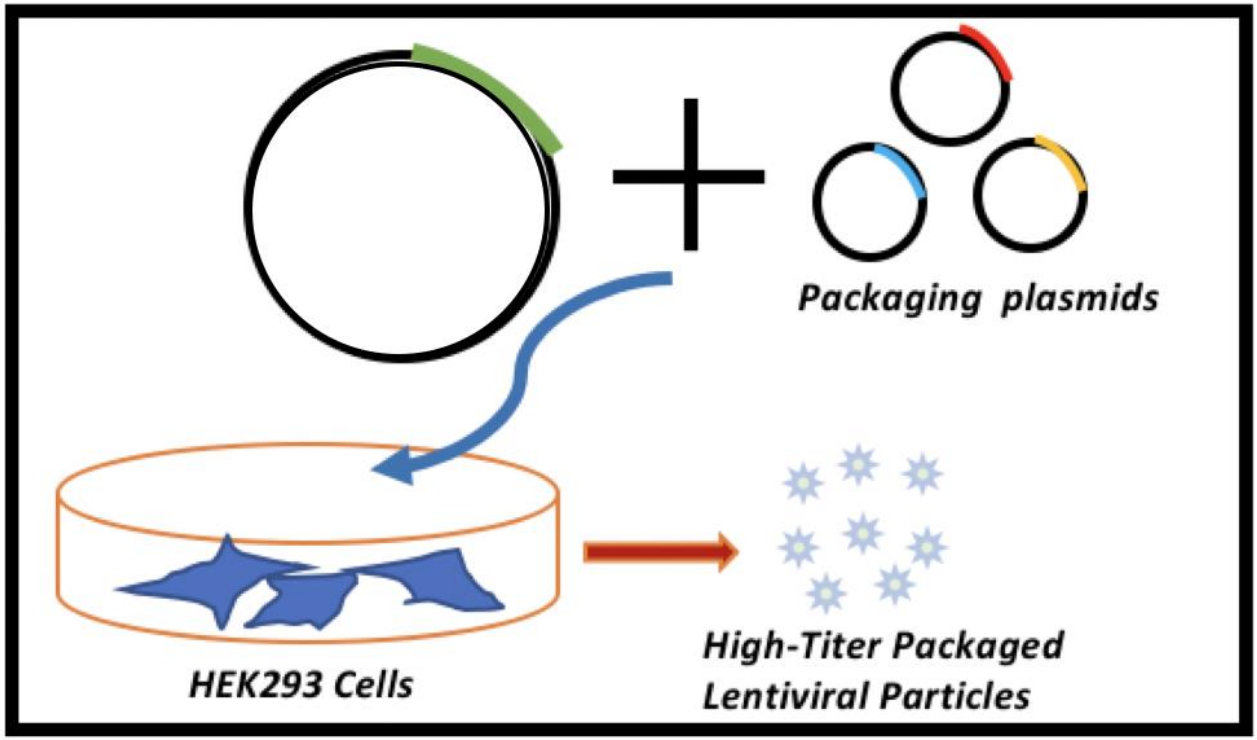

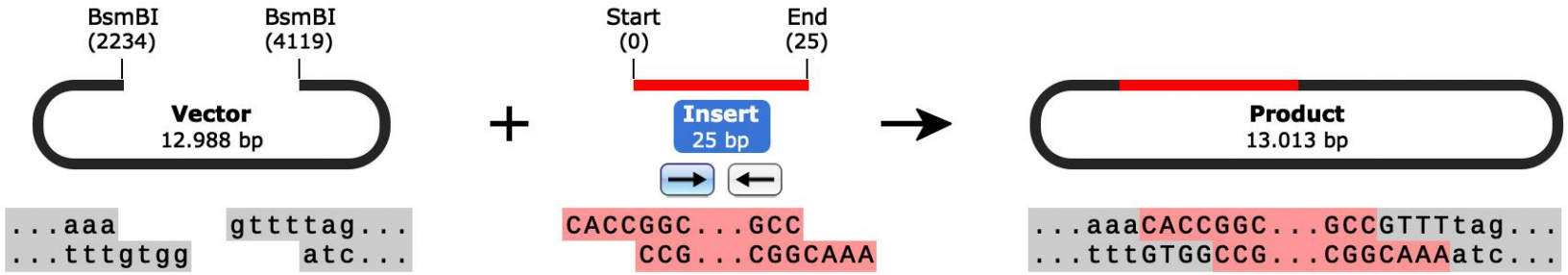

HLA-I Knock-Out via RNP

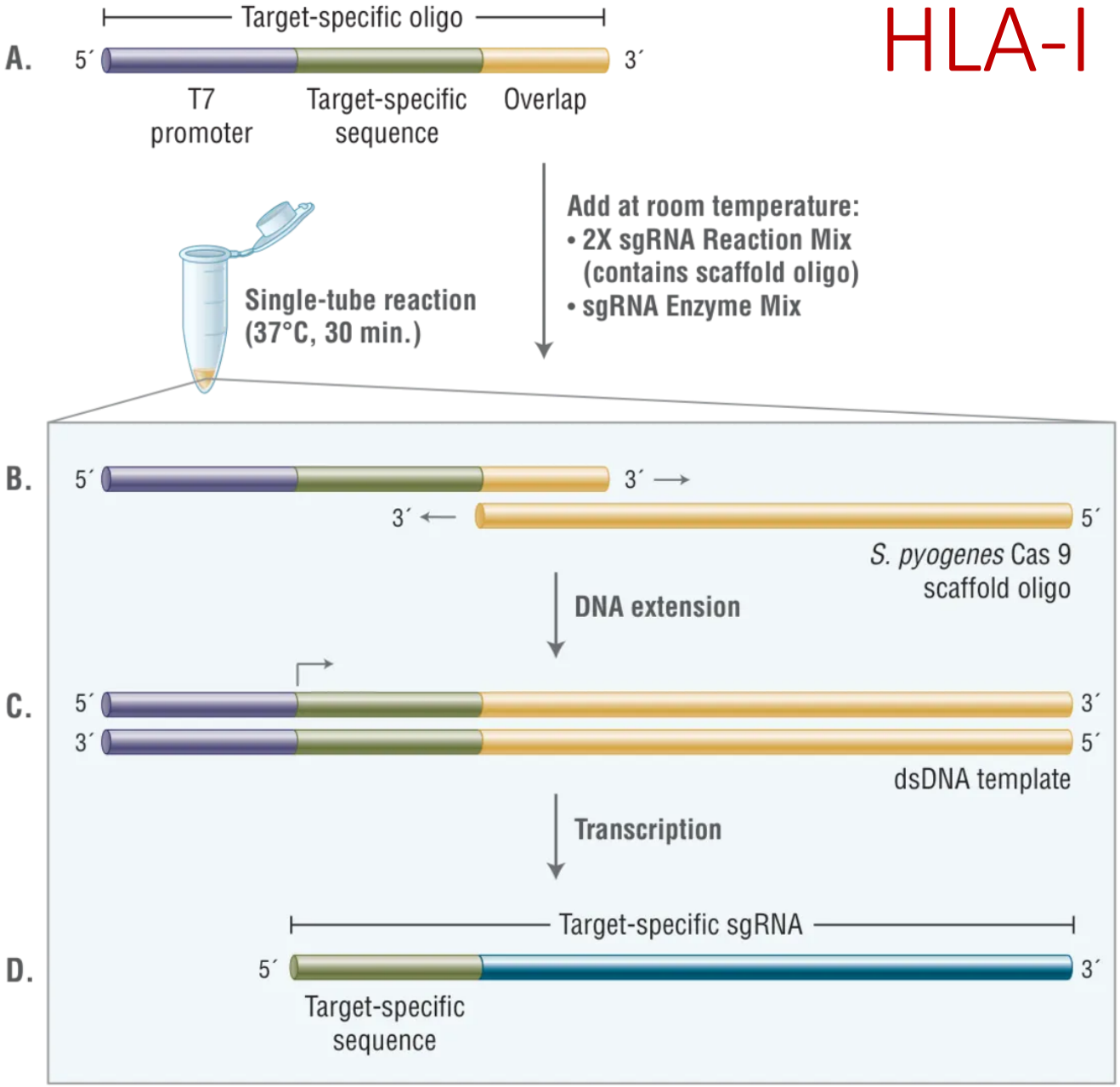

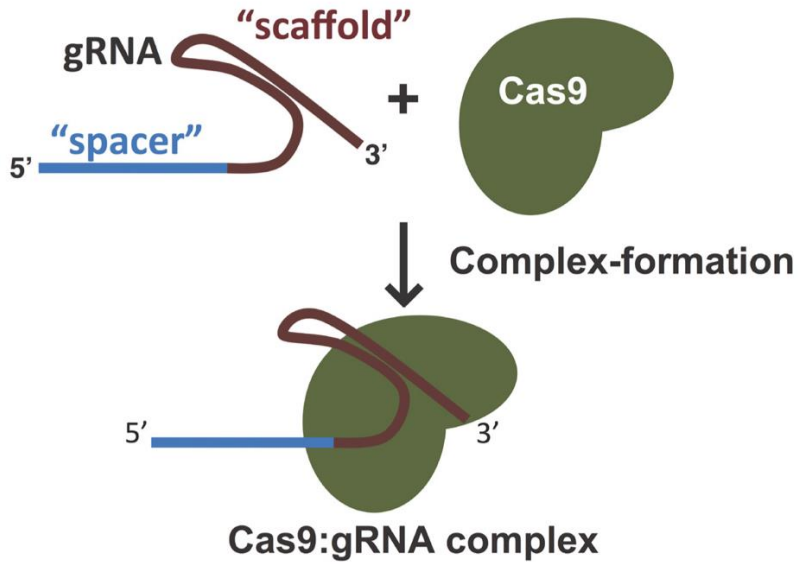

TTCTAATACGACTCACTATAGCTACTGAAGTATACGTAAAGGTTTT

HLA-I Knock-Out via RNP

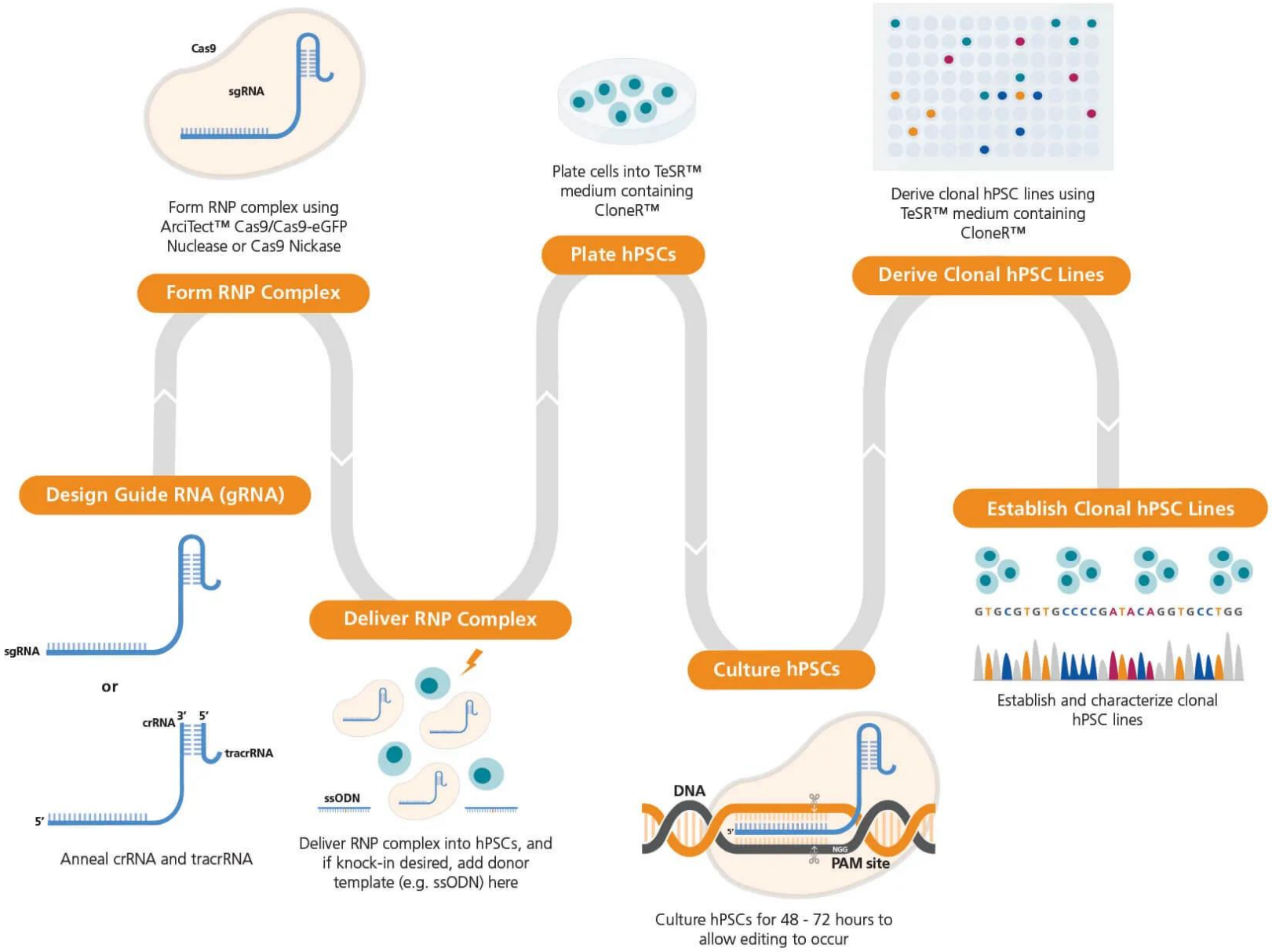

Guide RNA?
DNA’ yı kesmeden de düzenleyebiliriz!

Guide RNA?
DNA’ yı kesmeden de düzenleyebiliriz!

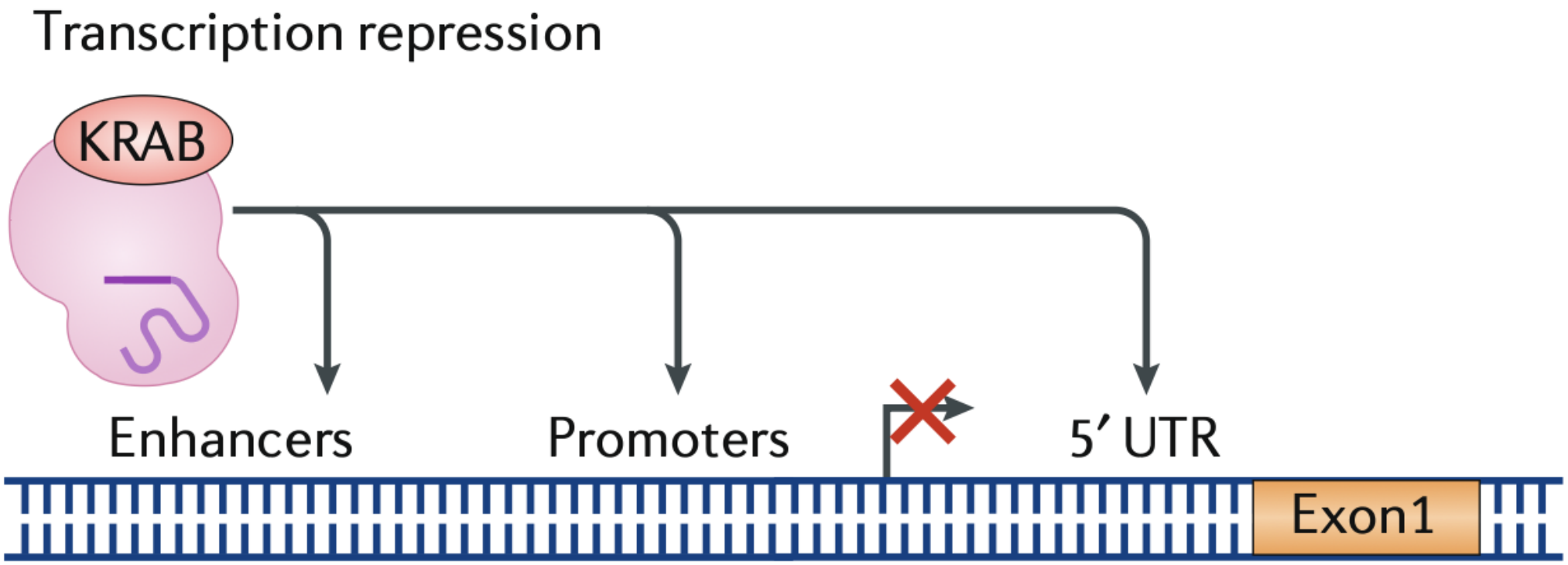

Pickar-Oliver et al., The next generation of CRISPR–Cas technologies and applications, Nature Reviews, 2019

Guide RNA?
DNA’ yı kesmeden de düzenleyebiliriz!

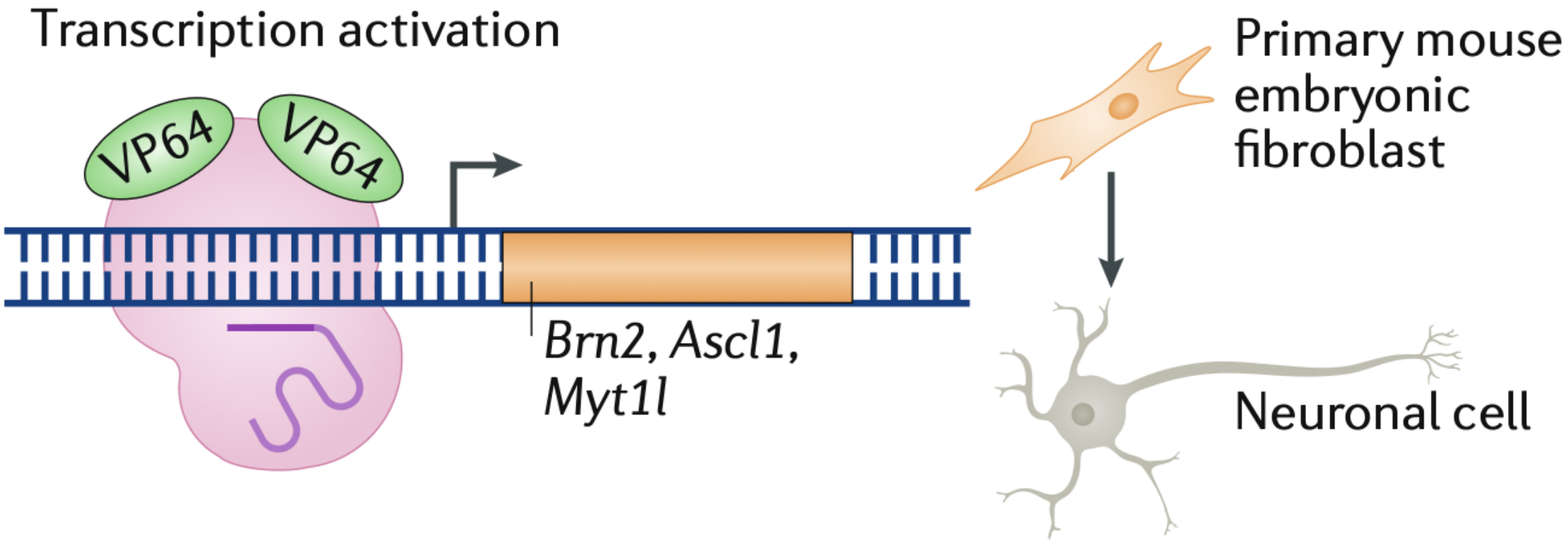

Pickar-Oliver et al., The next generation of CRISPR–Cas technologies and applications, Nature Reviews, 2019

Guide RNA?
DNA’ yı kesmeden de düzenleyebiliriz!

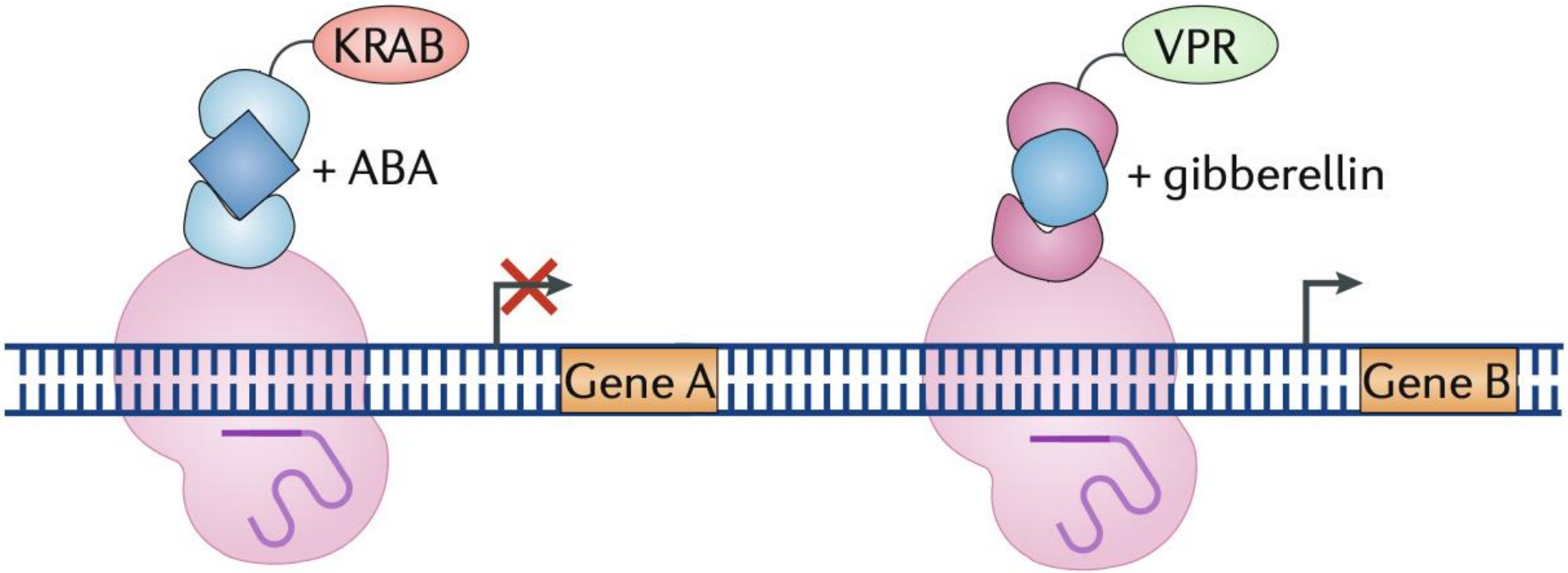

Pickar-Oliver et al., The next generation of CRISPR–Cas technologies and applications, Nature Reviews, 2019

Guide RNA?
DNA’ yı kesmeden de düzenleyebiliriz!

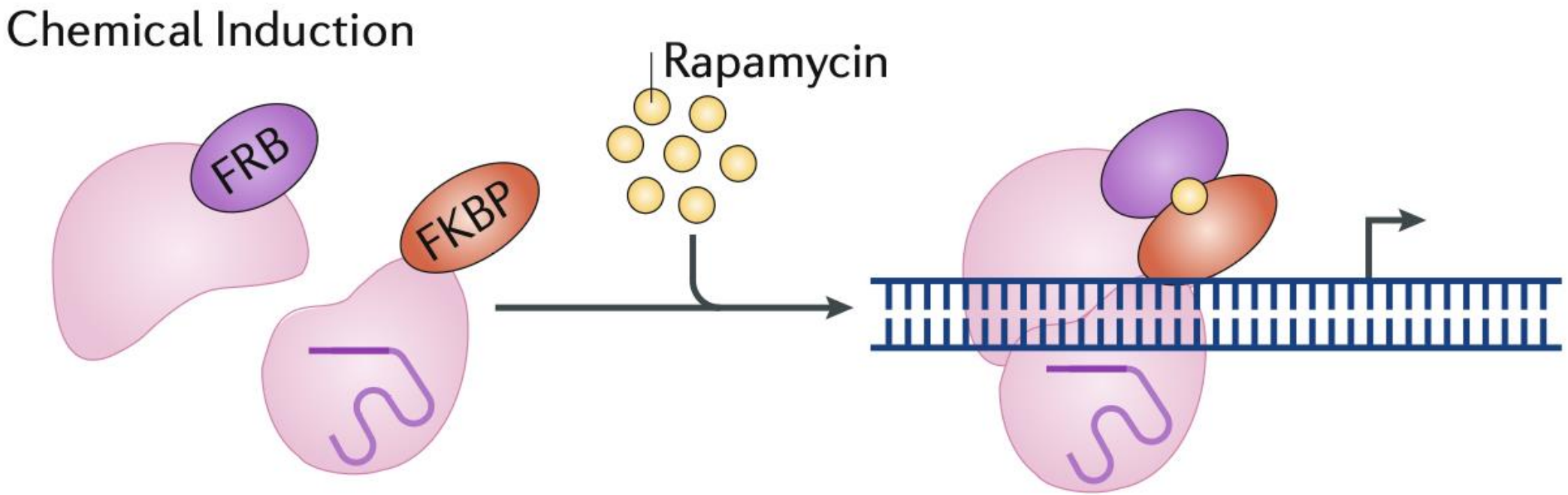

Pickar-Oliver et al., The next generation of CRISPR–Cas technologies and applications, Nature Reviews, 2019

Guide RNA?
DNA’ yı kesmeden de düzenleyebiliriz!

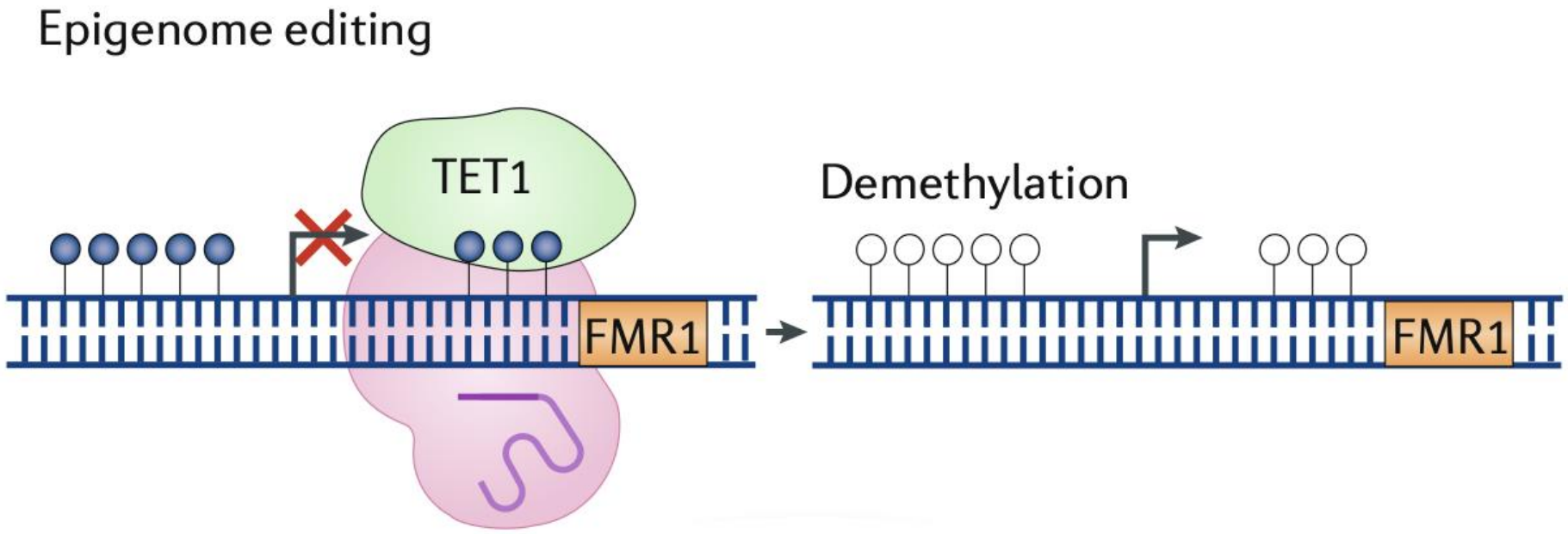

Pickar-Oliver et al., The next generation of CRISPR–Cas technologies and applications, Nature Reviews, 2019

Guide RNA?
DNA’ yı kesmeden de düzenleyebiliriz!

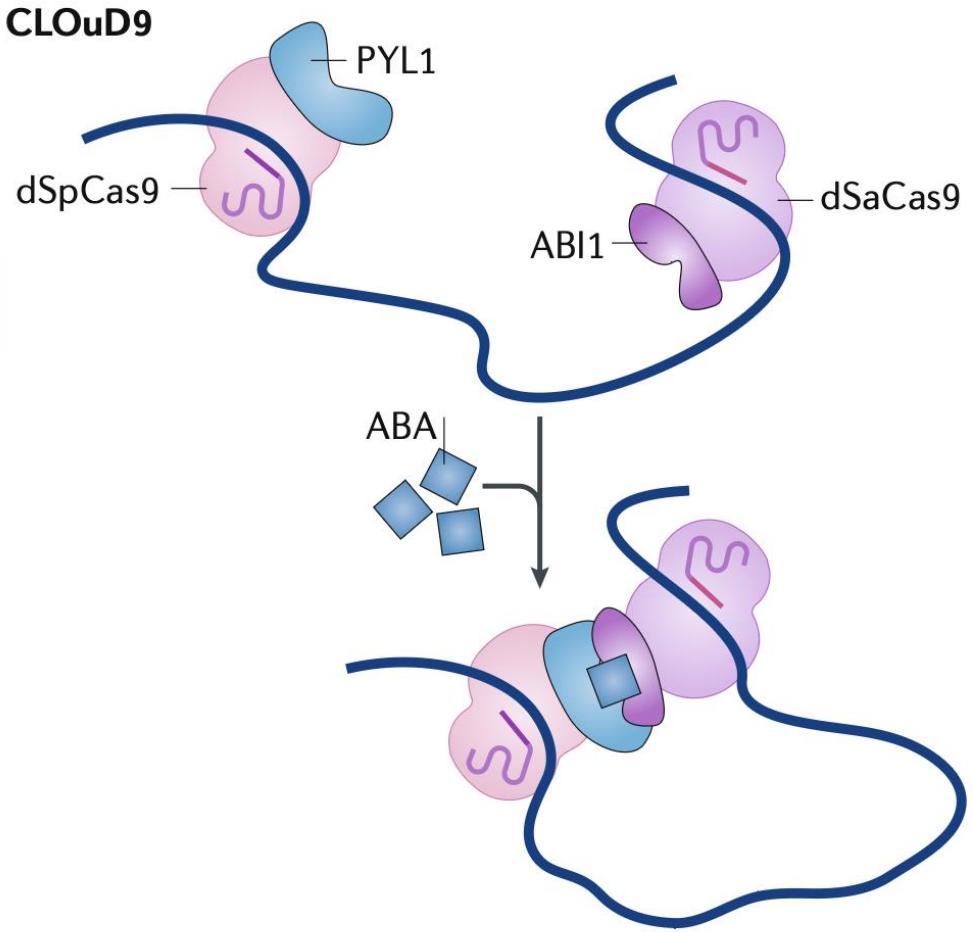

Pickar-Oliver et al., The next generation of CRISPR–Cas technologies and applications, Nature Reviews, 2019

casgevy®
(exagamglogene autotemcel)
suspension for IV infusion

Figure 5 **Therapeutic Hypothesis for *BCL11A* Gene Editing**

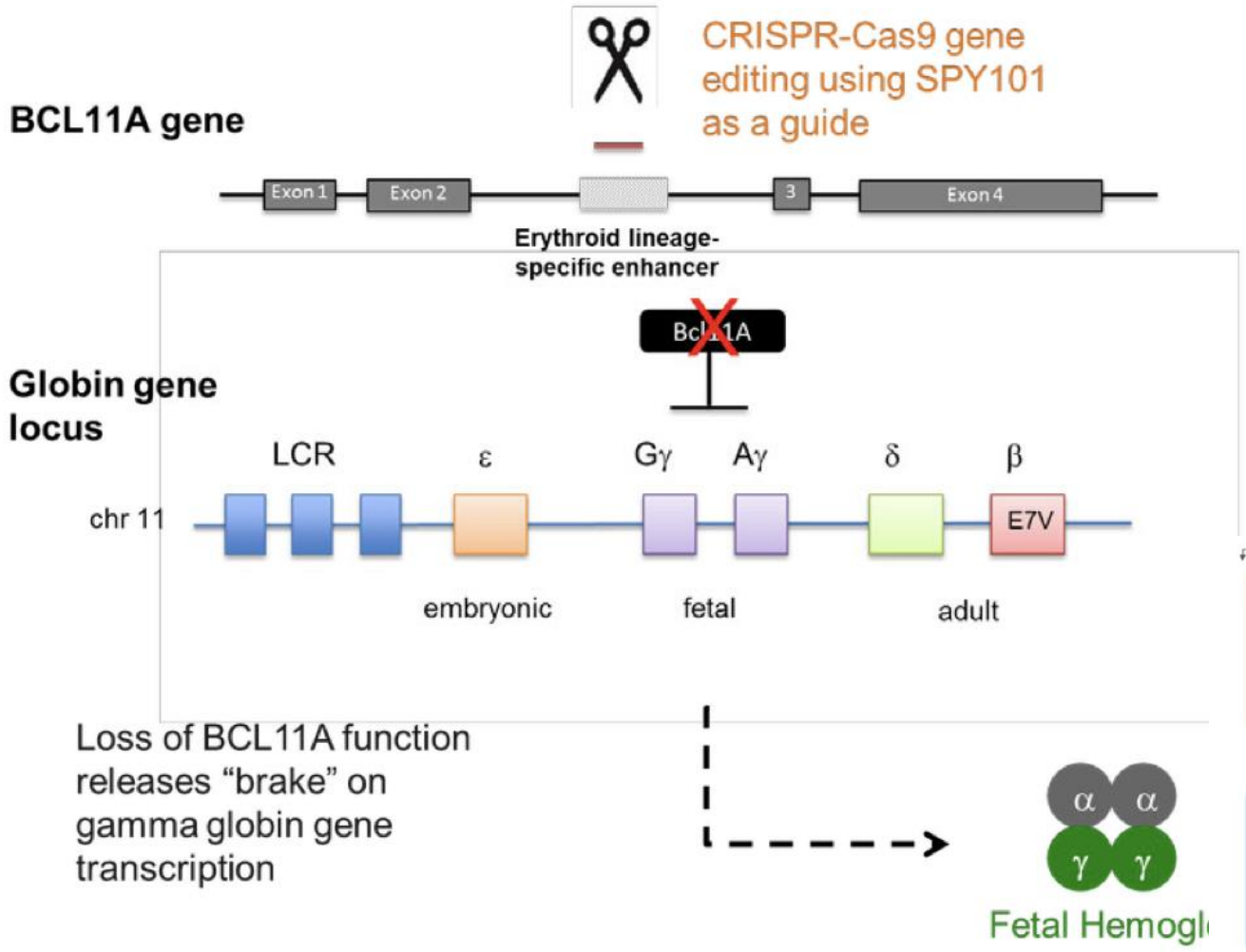

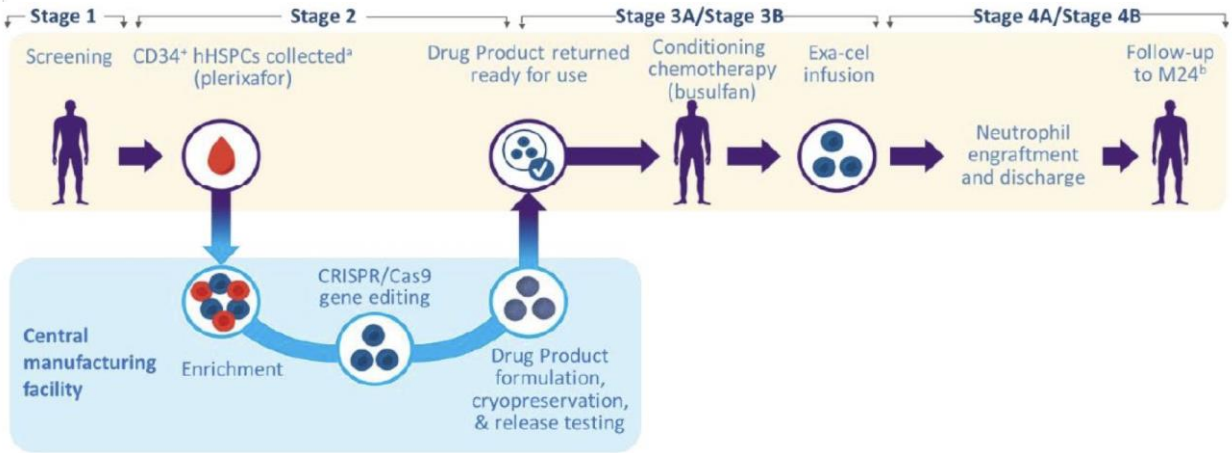

ORIGINAL ARTICLE

Exagamglogene Autotemcel for Severe Sickle Cell Disease

Authors: Haydar Frangoul, M.D., Franco Locatelli, M.D., Ph.D., Akshay Sharma, M.B., B.S., Monica Bhatia, M.D., Markus Mapara, M.D., Ph.D., Lyndsay Molinari, M.D., Donna Wall, M.D., +21, for the CLIMB SCD-121 Study Group* Author Info & Affiliations

Published April 24, 2024 | N Engl J Med 2024;390:1649-1662 | DOI: 10.1056/NEJMoa2309676
VOL. 390 NO. 18 | Copyright © 2024

Article | Open access | Published: 14 March 2025

Generation of hypoimmunogenic universal iPS cells through HLA-type gene knockout

Juryun Kim, Yoojun Nam, Doyeong Jeon, Yujin Choi, SeonJu Choi, Chang Pyo Hong, Siyoung Kim, Hyerin Jung, Narae Park, Yeowon Sohn, Yeri Alice Rim ✉ & Ji Hyeon Ju ✉

Experimental & Molecular Medicine **57**, 686–699 (2025) | Cite this article

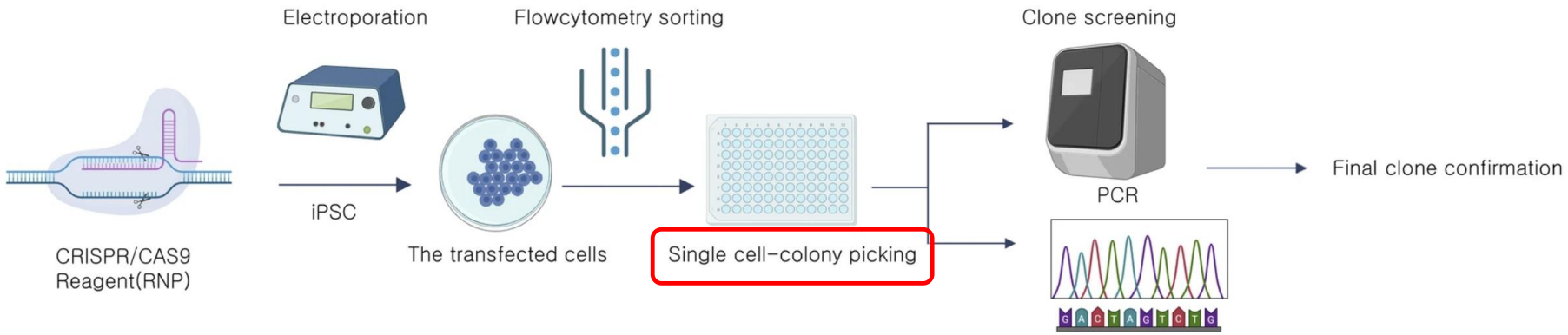

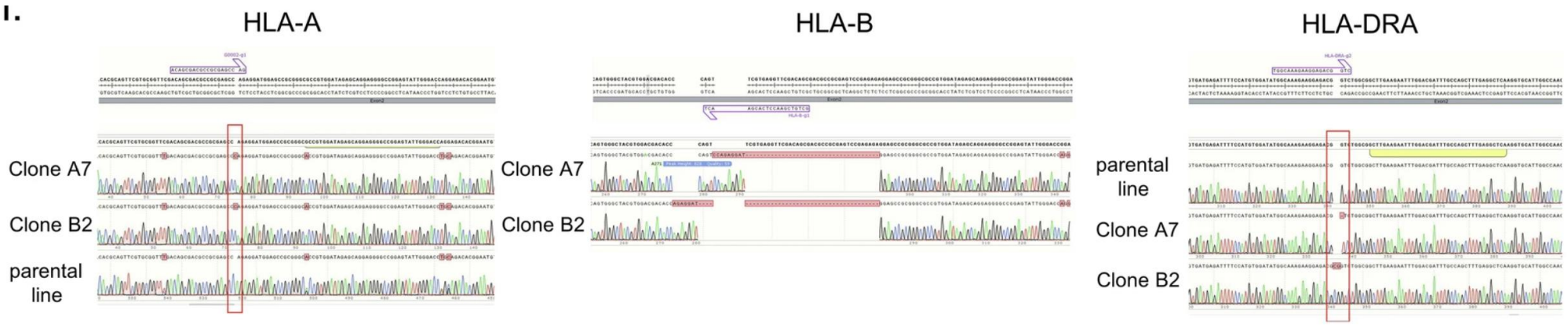

A Novel Platform for Creating Off-the-shelf Multiplex-Engineered Hematopoietic Cell Products

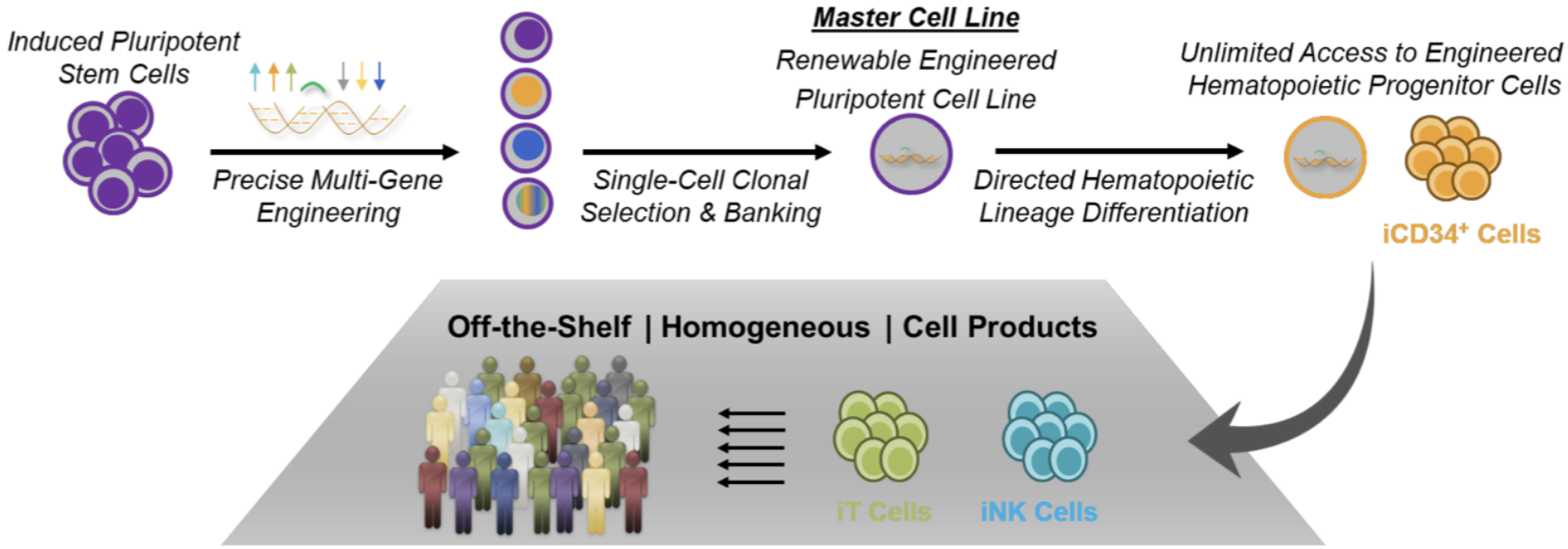

Fate THERAPEUTICS

Better Cells For Better Therapies™

Simultaneous Multi-Loci 2nd Round Engineering

Strategy 1:
Dual Loci Editing
CAR Knock-in at *B2M* and CIITA KO

Foundation Line

Strategy 2:
Triple Loci Editing
CAR Knock-in at Safe Harbor with B2M and CIITA KO

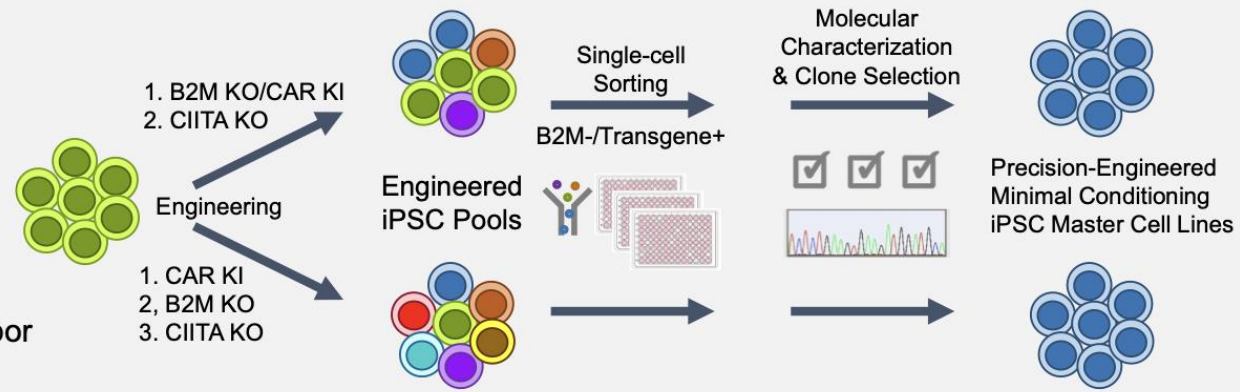

True Off-the-Shelf CAR T cell Drug Product

CAR19
State-of-the-art CAR motif and expression control

TCR null
Complete TCR knock-out to prevent GvHD in allogeneic settings

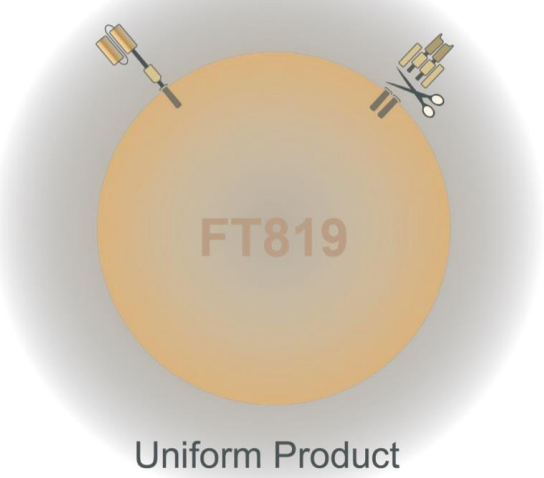

Uniform Product
Clonally engineered iPSC-derived CD8αβ T cell

CNTY-101 is an iPSC-derived NK cell therapy with CD19 CAR and Allo-Evasion™ edits to avoid host rejection

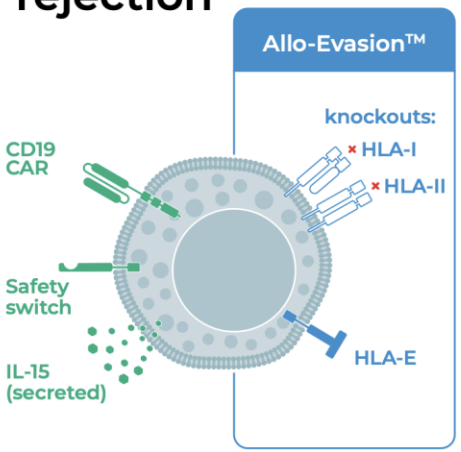

CNTY-101 is an allogeneic anti-CD19 iPSC-derived NK cell therapy

Century's technology for multiple step editing using CRISPR in iPSC allowed 6 edits (2 KO, 4 KI) to enable multiple functions

- Avoid host T cell rejection: Knockout of beta-2 microglobulin (b2M) and HLA Class II Transactivator (CIITA) to eliminate HLA-I & HLA-II
- Avoid host NK cell rejection: Knock-in of HLA-E
- Tumor elimination: CD19 CAR with FMC63 binder
- Safety switch: truncated Epidermal Growth Factor Receptor (EGFRt) containing Cetuximab binding epitope
- Secreted IL-15: to enhance cell persistence and modulate the tumor microenvironment

CNTY-101, an Allogeneic Anti-CD19 iPSC-Derived NK Product, for the Treatment of B Cell-Driven Autoimmune Diseases

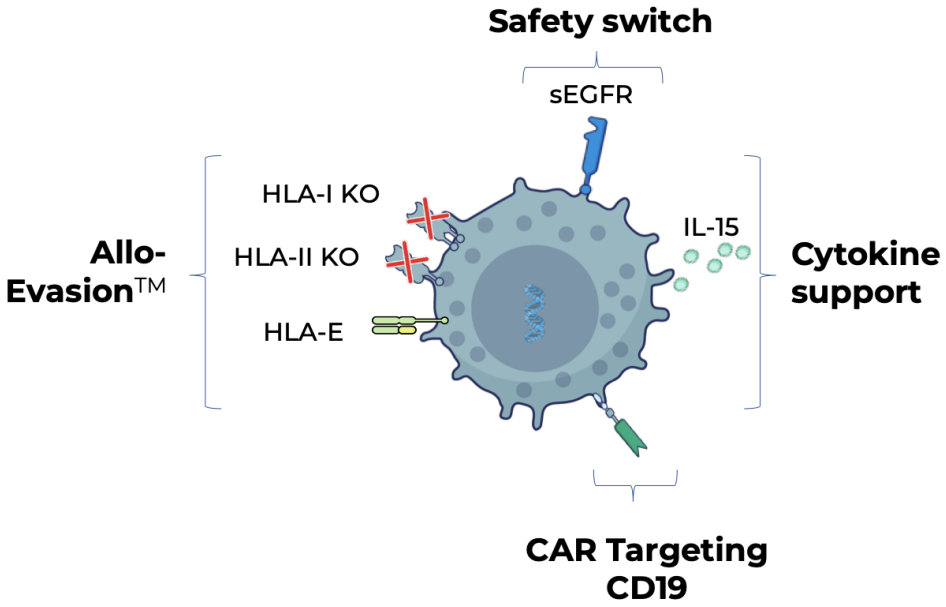

Allogenic iPSC-derived

- Available **'Off-the-Shelf'**
- No apheresis and no manufacturing wait time
- Clonal product enables batch-to-batch consistency

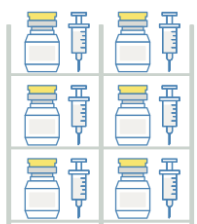

Drug product (iNK)

NK cells

- Killing potency (≥ primary CAR-T) leads to deep B-cell depletion[1]
- **Trafficking to secondary lymphoid tissues and marrow** favors pathogenic B-cell targeting
- Short-lived, more predictable pharmacokinetics and pharmacodynamics
- **Demonstrated efficacy, a manageable safety profile, and deep B cell depletion** in patients with (r/r) NHL (ELiPSE-1)

Allo-Evasion™

- **Avoiding host immune rejection**
- **Repeat dosing without continued lymphodepletion**
- Ability to re-treat, if needed

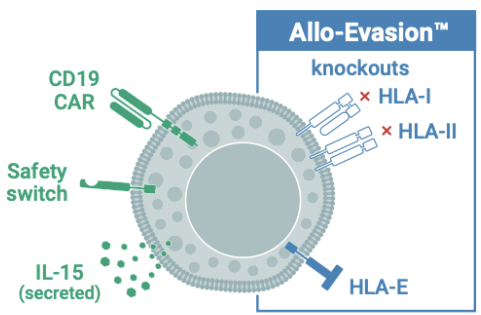

Tighter control over drug exposure:
B-cell depletion without prolonged B-cell aplasia

hin D et al, *Blood* 2004, 144: 3437

TEŞEKKÜRLER…